UNIVERSIDADE FEDERAL DE VIÇOSA

IGOR LIMA BRETAS

REMOTE SENSING APPLIED TO PASTURE MANAGEMENT

VIÇOSA - MINAS GERAIS
2022

IGOR LIMA BRETAS

REMOTE SENSING APPLIED TO PASTURE MANAGEMENT

Thesis submitted to the Animal Science Graduate Program of the Universidade Federal de Viçosa in partial fulfillment of the requirements for the degree of *Doctor Scientiae*.

Adviser: Fernanda Helena Martins Chizzotti

Co-advisers:

Domingos Sarvio Magalhães Valente

Fabyano Fonseca e Silva (*in memoriam*)

VIÇOSA - MINAS GERAIS
2022

Ficha catalográfica elaborada pela Biblioteca Central da Universidade Federal de Viçosa - Campus Viçosa

T
B844r
2022

Bretas, Igor Lima, 1993-
Remote sensing applied to pasture management / Igor Lima Bretas. – Viçosa, MG, 2022.
1 tese eletrônica (74 f.): il. (algumas color.).

Texto em inglês.
Inclui apêndices.
Orientador: Fernanda Helena Martins Chizzotti.
Tese (doutorado) - Universidade Federal de Viçosa, Departamento de Zootecnia, 2022.
Inclui bibliografia.
DOI: https://doi.org/10.47328/ufvbbt.2022.399
Modo de acesso: World Wide Web.

1. Pastagens - Manejo - Sensoriamento remoto. 2. Satélites artificiais em sensoriamento remoto. 3. Aprendizado do computador. 4. Vegetação - Índices. I. Chizzotti, Fernanda Helena Martins, 1977-. II. Universidade Federal de Viçosa. Departamento de Zootecnia. Programa de Pós-Graduação em Zootecnia. III. Título.

CDD 22. ed. 633.202

Bibliotecário(a) responsável: Alice Regina Pinto CRB6 2523

IGOR LIMA BRETAS

REMOTE SENSING APPLIED TO PASTURE MANAGEMENT

Thesis submitted to the Animal Science Graduate Program of the Universidade Federal de Viçosa in partial fulfillment of the requirements for the degree of *Doctor Scientiae*.

APPROVED: May 30, 2022

Assent:

Igor Lima Bretas
Author

Fernanda Helena Martins Chizzotti
Adviser

To my parents, Almir and Cecilia, for their constant effort, my brother Bruno for the unconditional support and my girlfriend Gabriela for her love and companionship.

I dedicate.

ACKNOWLEDGMENTS

To my parents for the example of dedication and for all the support given so that I managed to complete my goals;

To my brother for his friendship and motivation;

To my girlfriend, Gabriela, for her love, support, and for being part of the whole journey so far;

The Federal University of Viçosa and the Department of Animal Science, for opportunity for personal and professional development;

To Professor Fernanda Chizzotti for the opportunities, guidance, and support at every stage of my professional development;

To Professor Dilermando Miranda da Fonseca for all the fundamental teachings for my professional training;

To Professor Domingos Sárvio Magalhães Valente for all the support given during the development of this work;

To Professor Fabyano Fonseca e Silva (*in memoriam*) for the support and contribution to the enrichment of this work;

To Professor José Carlos B. Dubeux Jr. for the opportunity of professional development in the final stage of my doctorate;

To all the professors of the Department of Animal Science (UFV), for their knowledge transmitted;

To the Gefor-UFV team for their assistance in conducting this work;

To my friends from Viçosa, for all the help and moments of relaxation that made this journey easier;

To my friends and co-workers at the University of Florida – NFREC for all the support, friendship, and knowledge exchanged in the final stage of my doctorate;

To the Conselho Nacional de Desenvolvimento Científico e Tecnológico (CNPq), the Fundação de Amparo à Pesquisa do Estado de Minas Gerais (FAPEMIG) and to the Coordenação de Aperfeiçoamento de Pessoal de Nível Superior (CAPES) for granting the scholarship and for funding part of this research;

Finally, to all those who somehow helped me achieve this goal.

Thank you, so much!

"*Carry in your memory for the rest of your life the good things that emerged in the midst of difficulties. They will be proof of your ability to win the tests and will give you trust in the divine presence, which helps us in any situation, at any time, in the face of any obstacle*."

(Chico Xavier)

BIOGRAPHY

Igor Lima Bretas, son of Almir Ambrosio Bretas and Cecilia Muratori de Lima e Silva, was born in Muriae, Minas Gerais, on August 7th of 1993.

He joined the Animal Science undergrad at Universidade Federal de Viçosa in 2011 and received his bachelor's degree in 2016. In 2016, he started the Master's degree in the Department of Animal Science at the Universidade Federal de Viçosa, with major in Forages and Grasslands, concluding this degree in March of 2018. Then, he started his Ph.D. program in the same area and department, concluding the Ph.D. dissertation in May of 2022, after a period of research scholar program at the University of Florida, from January to August 2022.

ABSTRACT

BRETAS, Igor Lima, D.Sc., Universidade Federal de Viçosa, May, 2022. **Remote sensing applied to pasture management.** Adviser: Fernanda Helena Martins Chizzotti. Co-advisers: Domingos Sarvio Magalhães Valente and Fabyano Fonseca e Silva (*in memoriam*).

For this dissertation, two chapters were prepared based on the use of satellite images and machine learning techniques for automating pasture management. In the first chapter, we hypothesized that vegetation indexes (VIs) obtained through satellites providing moderate spatial resolution (Landsat-8 and Sentinel-2), combined with meteorological data, can accurately predict the aboveground biomass (AGB) of *Brachiaria* (syn. *Urochloa*) pastures in Brazil. We used AGB field data obtained from pastures between 2015 and 2019 in four distinct regions of Brazil to evaluate: (i) the relationship between three different VIs, normalized difference vegetation index (NDVI), enhanced vegetation index 2 (EVI2), and optimized soil adjusted vegetation index (OSAVI), and meteorological data with pasture aboveground fresh biomass (AFB), aboveground dry biomass (ADB), and dry matter concentration (DMC); and (ii) performance of simple linear regression (SLR), multiple linear regression (MLR) and random forest (RF) algorithms for the prediction of pasture AGB based on VIs obtained through satellite imagery combined with meteorological data. The results highlight a strong correlation (r) between VIs and AGB, particularly NDVI (r = 0.52 to 0.84). The MLR and RF algorithms demonstrated high potential to predict AFB (R^2 = 0.76 to 0.85) and DMC (R^2 = 0.78 to 0.85). We conclude that both MLR and RF algorithms improved the biomass prediction accuracy using satellite imagery combined with meteorological data to determine AFB and DMC, and can be used for *Brachiaria* (syn. *Urochloa*) AGB prediction. In the second chapter, we aimed to develop a model for automated height classification and evaluate the accuracy of indirect estimates of forage biomass in Mombaça guinea grass (*Megathyrsus maximus* cv. Mombaça) pastures. This model is based on the analysis of images obtained through the Sentinel-2 satellite using machine learning techniques to support decision-making regarding grazing management and stocking rate adjustment. We used different bands from the Sentinel-2 satellite that were obtained and processed entirely in the cloud. Three forage height classes were previously defined as class 0 (<45cm), class 1 (45–80cm) and class 2 (>80cm) according to management recommendations. The random forest algorithm was used to classify forage height and predict biomass by using height and biomass field data obtained from 54 paddocks in Brazil between

2016 and 2018 as reference data. The results demonstrate precision, recall, and accuracy values of up to 83, 90, and 83%, respectively, for paddock height classification and the potential to accurately predict AFB and DMC (R^2=0.69 and 0.82, respectively). We conclude that the combined use of satellite imagery and machine learning techniques makes it possible to classify height and predict the biomass of Mombaça guinea grass (*Megathyrsus maximus* cv. Mombaça) accurately while supporting decision-making regarding grazing management and stocking adjustment. However, more studies must be carried out to improve the models proposed in both chapters and more efforts must be made to implement the tool under field conditions.

Keywords: Machine learning. Remote sensing. Satellites. Vegetation indices.

RESUMO

BRETAS, Igor Lima, D.Sc., Universidade Federal de Viçosa, maio de 2022. **Sensoriamento remoto aplicado ao manejo de pastagens.** Orientadora: Fernanda Helena Martins Chizzotti. Coorientadores: Domingos Sarvio Magalhães Valente e Fabyano Fonseca e Silva (*in memoriam*).

Para esta tese, dois capítulos foram elaborados baseados no uso de imagens de satélites e técnicas de aprendizagem de máquinas para automatização do manejo de pastagens. No primeiro capítulo foi levantada a hipótese de que índices de vegetação (IV) obtidos por meio de satélites de moderada resolução espacial (Landsat-8 e Sentinel-2), combinados com dados meteorológicos, podem prever com acurácia a biomassa de forragem em pastagens de *Brachiaria* (sin. *Urochloa*) no Brasil. Foram usados dados de biomassa obtidos a campo entre os anos de 2015 e 2019 em quatro regiões distintas do Brasil para avaliar: (i) a relação entre três diferentes IV e dados meteorológicos com biomassa fresca (BF), biomassa seca (BS) e concentração de matéria seca (CMS); e (ii) o desempenho dos algoritmos de regressão linear simples (RLS), regressão linear múltipla (RLM) e random forest (RF) para a predição da biomassa de forragem. Os resultados destacam forte correlação (r) entre IV e BF, principalmente NDVI (r = 0,52 a 0,84). Os algoritmos RLM e RF demonstraram alto potencial para predizer BF (R^2 = 0,76 a 0,85) e CMS (R^2 = 0,78 a 0,85). Foi concluído que os algoritmos RLM e RF melhoraram a acurácia de previsão da biomassa usando imagens de satélite combinadas com dados meteorológicos, e podem ser usados para a previsão da biomassa em pastos de *Brachiaria* (sin. *Urochloa*). No segundo capítulo o objetivo foi desenvolver um modelo para classificação automatizada da altura e avaliar a acurácia das estimativas indiretas da biomassa de forragem em pastagens de *Panicum maximum* cv. Mombaça (sin. *Megathyrsus maximus* cv. Mombaça). Este modelo baseia-se na análise de imagens obtidas através do satélite Sentinel-2 utilizando técnicas de aprendizado de máquinas para suportar a tomada de decisão quanto ao manejo do pastejo e ajustes da taxa de lotação. Foram utilizadas diferentes bandas do satélite Sentinel-2 que foram obtidas e processadas inteiramente em nuvem. Três classes de altura do pasto foram previamente definidas como classe 0 (<45cm), classe 1 (45–80cm) e classe 2 (>80cm) de acordo com as recomendações de manejo do capim-mombaça. O algoritmo RF foi usado para classificar a altura do pasto e prever a biomassa usando dados de altura e biomassa obtidos a campo em 54 piquetes no Brasil entre os anos 2016 e 2018 como dados de referência. Os resultados demonstram valores de precisão, sensibilidade e acurácia de até 83,

90 e 83%, respectivamente, para classificação da altura do piquete e potencial para prever a BF e CMS do pasto (R^2 = 0,69 e 0,82, respectivamente). Conclui-se que o uso combinado de imagens de satélite e técnicas de aprendizado de máquina possibilita classificar a altura e prever a biomassa de *Panicum maximum* cv. Mombaça (sin. *Megathyrsus maximus* cv. Mombaça) com acurácia, suportando a tomada de decisão quanto ao manejo do pastejo e ajustes das taxas de lotação. No entanto, mais estudos devem ser realizados para melhorar os modelos propostos em ambos os capítulos e mais esforços devem feitos para implementação da ferramenta em condições de campo.

Palavras-chave: Aprendizagem de máquinas. Índices de vegetação. Satélites. Sensoriamento remoto.

SUMMARY

General introduction

The growing global concern about food supply, traceability, environmental impacts, and economic factors makes it necessary to increase the production efficiency in animal production systems. The main challenge to attaining the world demand is to overcome the low monitoring capacity and data collection, mainly because of the tendencies of increasing number of animals, decreasing number of farms, and decreasing labor offer in the field in a global scenario (Berni et al. 2006; ABIEC 2020; Ellis et al. 2020). The concentration of activities per worker in field conditions prevents the continuous collection of data, essentials for decision-making in animal production systems.

New technologies are essential tools for livestock management allowing the monitoring of animals and pastures remotely and automatically. In this context, Precision Livestock Farming, which uses real-time monitoring technologies, can be applied to manage animals or the environment in which they are raised at an individual level (Halachmi and Guarino, 2016). In terms of grazing systems, knowing the pasture biomass and canopy height are fundamental to improving the management and increasing the system's efficiency and sustainability. However, continuous monitoring of the spatial and temporal variability at a paddock level is laborious and sometimes impossible by humans. To solve this problem, advances have been achieved in recent years of research using remote sensing to manage pasture as highlighted in recent literature reviews (Reinermann et al. 2020; Murphy et al. 2021). Sensors aboard drones or proximal sensors are useful and recommended for areas that require high spatial resolution or in places where the cloud cover is frequent. However, they require the presence of an operator in the field and are restricted to small areas. On the otherhand, images from several satellites are available for free and useful for large area sensing, allowing remote monitoring. Grassland areas are frequently of great extension and difficult to access, justifying the interest in satellites use for pastures management automatization.

Although sensors allow the data collection in large scale, sensor-based data are generated on a large volume, high speed and in different formats, creating a “big data” that exceeds the capacity of analysis by traditional tools (Morota et. al 2018). Artificial intelligence has been increasingly employed in recent years to address the challenge of complexity and non-linearity of the data (Ali et al. 2015; Morota et al. 2018). Among the primary tools used in artificial intelligence, machine learning techniques have gained prominence due to the capacity to automatize the big data analysis with a good performance. Different machine learning

algorithms can recognize patterns in complex datasets and solve several regression or classification problems quickly and automatically.

Some of the main variables associated with pasture management are forage biomass and canopy height because they are directly linked to stocking rate adjustments and grazing management. In this dissertation, field datasets from different regions were used as reference data to develop models applied to pasture management using machine learning, specifically supervised learning techniques. We developed one model for biomass prediction in *Brachiaria spp*. (syn. *Urochloa*) pastures and other two models for biomass prediction and height classification in Mombaça guinea grass (*Megathyrsus maximus* cv. Mombaça), the main grasses used in continuous and rotational stocking systems, respectively, in Brazil.

References

Ali, I., Greifeneder, F., Stamenkovic, J., Neumann, M., & Notarnicola, C., 2015. Review of Machine Learning Approaches for Biomass and Soil Moisture Retrievals from Remote Sensing Data. *Remote Sensing*, *7*(12), 16398–16421. https://doi.org/10.3390/rs71215841

Associação Brasileira das indústrias exportadoras de carne – ABIEC (Brazilian Beef Exporters Association). 2020. Available online at: http://abiec.com.br/en/publicacoes/beef-report-2020-2/

Berni, D. A.; Marquetti, A.; Peixoto, F. C. 2006. Evolução setorial da economia brasileira entre 2002 e 2020: do passado ao futuro com o método Delphi (Sectorial evolution of the Brazilian economy between 2002 and 2020: from the past to the future with the Delphi method). Análise Econômica (UFRGS), v. 24, p. 183-210.

Ellis, J., DeLong, K. L., Lambert, D. M., Schexnayder, S., Krawczel, P., & Oliver, S. (2020). Analysis of closed versus operating dairies in the southeastern United States. *Journal of Dairy Science*, *103*(6), 5148–5161. https://doi.org/10.3168/jds.2019-17516

Halachmi, I.; Guarino, M., 2016. Editorial: Precision Livestock Farming: A 'per Animal' Approach Using Advanced Monitoring Technologies. *Animal*, 10, 1482–1483. https://doi.org/10.1017/S1751731116001142

Morota G.; Ventura R. G., Silva F. F., Koyama M., Fernando S. C., 2018. Machine learning and data mining advance predictive big data analysis in precision animal. *Journal of Animal Science*, 96:1540–1550. https://doi.org/10.1093/jas/sky014

Murphy, D.J., Murphy, M.D., O'Brien, B., O'Donovan, M., 2021. A Review of Precision Technologies for Optimising Pasture Measurement on Irish Grassland. *Agriculture* 11, 600. https://doi.org/10.3390/agriculture11070600

Reinermann, S., Asam, S., Kuenzer, C., 2020. Remote Sensing of Grassland Production and Management—A Review. *Remote Sensing*, 12, 1949. https://doi.org/10.3390/rs1212194

CHAPTER 1- Prediction of aboveground biomass and dry matter concentration in *Brachiaria* pastures by combining meteorological data and satellite imagery.

Article published in Grass and Forage Science (2021). https://doi.org/10.1111/gfs.12517

Graphical abstract

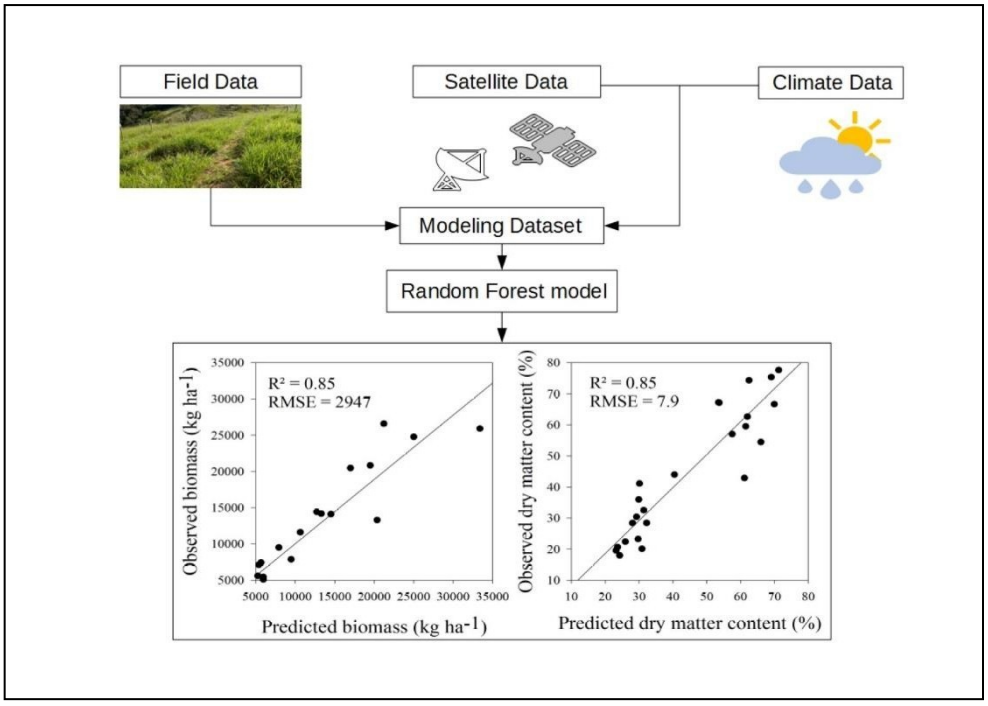

Abstract

Aboveground biomass (AGB) data are important for profitable and sustainable pasture management. In the present study, we hypothesized that vegetation indexes (VIs) obtained through satellites providing moderate spatial resolution (Landsat-8 and Sentinel-2), combined with meteorological data, can accurately predict the AGB of *Brachiaria spp*. (syn. *Urochloa*) pastures in Brazil. We used AGB field data obtained from pastures between 2015 and 2019 in four distinct regions of Brazil to evaluate: (i) the relationship between three different VIs, normalized difference vegetation index (NDVI), enhanced vegetation index 2 (EVI2), and optimized soil adjusted vegetation index (OSAVI), and meteorological data with pasture aboveground fresh biomass (AFB), aboveground dry biomass (ADB), and dry matter concentration (DMC); and (ii) performance of simple linear regression (SLR), multiple linear regression (MLR) and random forest (RF) algorithms for the prediction of pasture AGB based

on VIs obtained through satellite imagery combined with meteorological data. The results highlight a strong correlation (r) between VIs and AGB, particularly NDVI (r = 0.52 to 0.84). The MLR and RF algorithms demonstrated high potential to predict AFB (R^2 = 0.76 to 0.85) and DMC (R^2 = 0.78 to 0.85). We conclude that both MLR and RF algorithms improved the biomass prediction accuracy using satellite imagery combined with meteorological data to determine AFB and DMC, and can be used for *Brachiaria* (syn. *Urochloa*) AGB prediction. Additional research on tropical grasses is needed to evaluate different VIs improving the accuracy of ADB prediction, thereby supporting pasture management in Brazil.

KEYWORDS

Biomass. Machine learning. Remote sensing. Satellite. Tropical grasslands. Vegetation index.

1 | INTRODUCTION

Grasslands occupy the majority of global agricultural lands and play essential roles in livestock production systems worldwide (Li et al., 2015). In Brazil, pastures occupy approximately 160 million hectares (IBGE, 2017). Most national livestock systems are based on pastures of tropical grasses, mainly *Brachiaria* (syn. *Urochloa*), thereby making management of this type of grasslands essential for profitability and sustainability. The genus *Brachiaria* (syn. *Urochloa*) comprises 85% of cultivated pastures in Brazil (Jank et al., 2014). In general, are cultivated in Brazil because of its high resistance to acid soils, low fertility and good productive potential in the rainy season (Machado et al., 2020).

Aboveground biomass (AGB) knowledge is essential for adjusting stocking rates and grazing cycles, as overgrazing or sub-grazing conditions causes soil degradation, compromise perenniality and reduces the harvest efficiency of the forage (de Oliveira et al., 2004; Carnevalli et al., 2006; Santos et al., 2013). The traditional methodologies used to quantify pasture AGB are based on obtaining pasture samples by cutting within frames encompassing a known area, followed by weighing and laboratory analysis (Sanderson et al., 2001; Barbero et al., 2015; Delevatti et al., 2019). However, at the field level, this pasture monitoring method is laborious, time-consuming, and expensive. In addition, pasture areas often show considerable soil, relief, and species heterogeneity. Therefore, the AGB quantification by direct cutting, besides being

destructive, often does not represent the spatial variability of the area, which reduces the accuracy of the collected data.

Currently, one technology used in the pasture management improvement is remote sensing (RS). Several studies have demonstrated the potential of RS for leaf area index (LAI), height and AGB estimates of pasture. Batistoti et al. (2019) and Lussem et al. (2019) used unmanned aerial vehicles (UAV) for biomass and canopy height estimates in Brazilian and temperate grassland, respectively. Insua et al. (2019) also used UAV to estimate the spatial and temporal variability of pasture growth and digestibility, while Wijesingha et al. (2020) used UAV equipped with a hyperspectral camera to access the crude protein (CP) and acid detergent fiber (ADF) content of forage in eight different pasture areas in Germany, demonstrating that it is also possible to use RS to monitor forage nutritive value. Similarly, Edirisinghe et al. (2012), Wang et al. (2017), Punalekar et al. (2018), and Otgonbayar et al. (2019) demonstrated the satellite data potential to predict pasture biomass in New Zealand, China, England, and Mongolia, respectively. Wang et al. (2019) also demonstrated reasonably prediction of the seasonal dynamics and spatial heterogeneity of LAI and AGB by satellite-based RS in USA. The main limitations of satellite-based RS are low temporal resolution and frequent cloud coverage. The combined use of Landsat-8 and Sentinel-2 satellites offers possibility for free, high-frequency and long-term pastures monitoring. Mandanici et al. (2016) compared images obtained by the Landsat-8 and Sentinel-2 satellites in different study areas and found strong correlations and high regression coefficients between all corresponding bands and spectral indices calculated with the different sensors, indicating that both satellites can be well combined. Wang et al. (2019) and Chakhar et al. (2020) also demonstrated the possibility of combining Landsat-8 and sentinel-2 images to improve the accuracy of pasture biomass estimates and crop classification, respectively.

Tong et al. (2019) used different vegetation indexes (VIs) obtained through a proximal sensor to predict pasture biomass at peak production. Several other recent studies have demonstrated that VIs are accurate in predicting pasture AGB and can be used in pasture monitoring (Otgonbayar et al., 2019; Hill et al., 2017; Michez et al., 2019; Guerini Filho et al., 2020). The NDVI (normalized difference vegetation index) is the most widely used VI for monitoring crops and pastures; however, this index loses sensitivity in areas of high biomass and leaf area index or the presence of exposed soil patches in the pasture. Several other indices have been proposed to minimize these problems (Gitelson and Merzlyak, 1994; Liu and Huete,

1995; Rondeaux et al., 1996; Mutanga and skidmore, 2004; Jiang et al., 2008; Gu et al., 2013 and Fern et al., 2018).

Brazilian pastures are predominantly formed by grasses of the genus *Brachiaria* (syn. *Urochloa*) and are characterized by high spatial variability in terms of canopy structure, ground cover and relief. In addition, the grass growth pattern demonstrates great temporal variability in response to changes in weather conditions (i.e., precipitation, temperature, radiation, etc.), requiring additional studies combining spectral and meteorological data to predict the AGB of these pastures in the tropical region (Santana et al., 2016; Fontana et al., 2018; Terra et al., 2020). The development of methodologies that provide highly accurate, low cost, and timely information is vital for decision-making within farm management. In this context, several methods have been proposed to potentially improve AGB prediction accuracy, such as regression models and machine learning tools, and the latter has been particularly successful in increasing the AGB prediction accuracy due to their ability to process large numbers of inputs and work with non-linear problems (Ali et al., 2015). Among machine learning methods, the random forest (RF) algorithm, which is a combination of multiple decision trees, has substantial promise for grassland biomass prediction because it is fast, potentially more effective than traditional regression approaches (Idowu et al., 2016), and requires fewer training samples than the artificial neural networks (ANN) method (Ali et al., 2015). In summary, RF combines the base principles of bagging with random feature selection to add additional diversity to the decisions of the predictive models.

In the present study, we hypothesized that VIs obtained through satellites providing moderate spatial resolution (Landsat-8 and Sentinel-2), combined with meteorological data, can accurately predict the AGB of *Brachiaria* (syn. *Urochloa*) pastures in Brazil. We used pasture AGB data obtained in the field between 2015 and 2019 in four different regions of Brazil. We evaluated (i) the relationships between three different VIs and meteorological data with pasture aboveground fresh biomass (AFB), aboveground dry biomass (ADB), and dry matter concentration (DMC); and (ii) performance of simple linear regression (SLR), multiple linear regression (MLR) with backward elimination and RF algorithm with variable selection in the prediction of pasture AGB based on VIs obtained using satellite imagery combined with meteorological data to determine which method is the more robust and accurate for our study conditions.

2 | MATERIALS AND METHODS

2.1 | Study areas

Field sampling for the AGB calculation was conducted in forty total paddocks: twenty-four owned by the Unidade de Ensino, Pesquisa e Extensão em Gado de Corte (UEPE-GC) of the Universidade Federal de Viçosa, in Minas Gerais (Field 1), five owned by Embrapa Gado de Leite, in Coronel Pacheco-MG (Field 2), eight located in Patrocínio Paulista – SP (Field 3), and three owned by Embrapa Agrossilvipastoril, located in Sinop-MT (Field 4). Figure 1 shows study area locations, and Table 1 provides pasture details. The four experimental areas were located in three Brazilian biomes, with different weather characteristics, and were formed predominantly (over 90%) by species of the genus *Brachiaria* (syn. *Urochloa*). According to Köppen's classification, the climate type of the field 1 and field 2 is Cwa (mesothermal), field 3 fits the Aw type and field 4 has a monsoon Am climate. The paddocks covered a total area of approximately 164 ha of pasture and the four areas were monitored between the summer of 2015 and the summer of 2019.

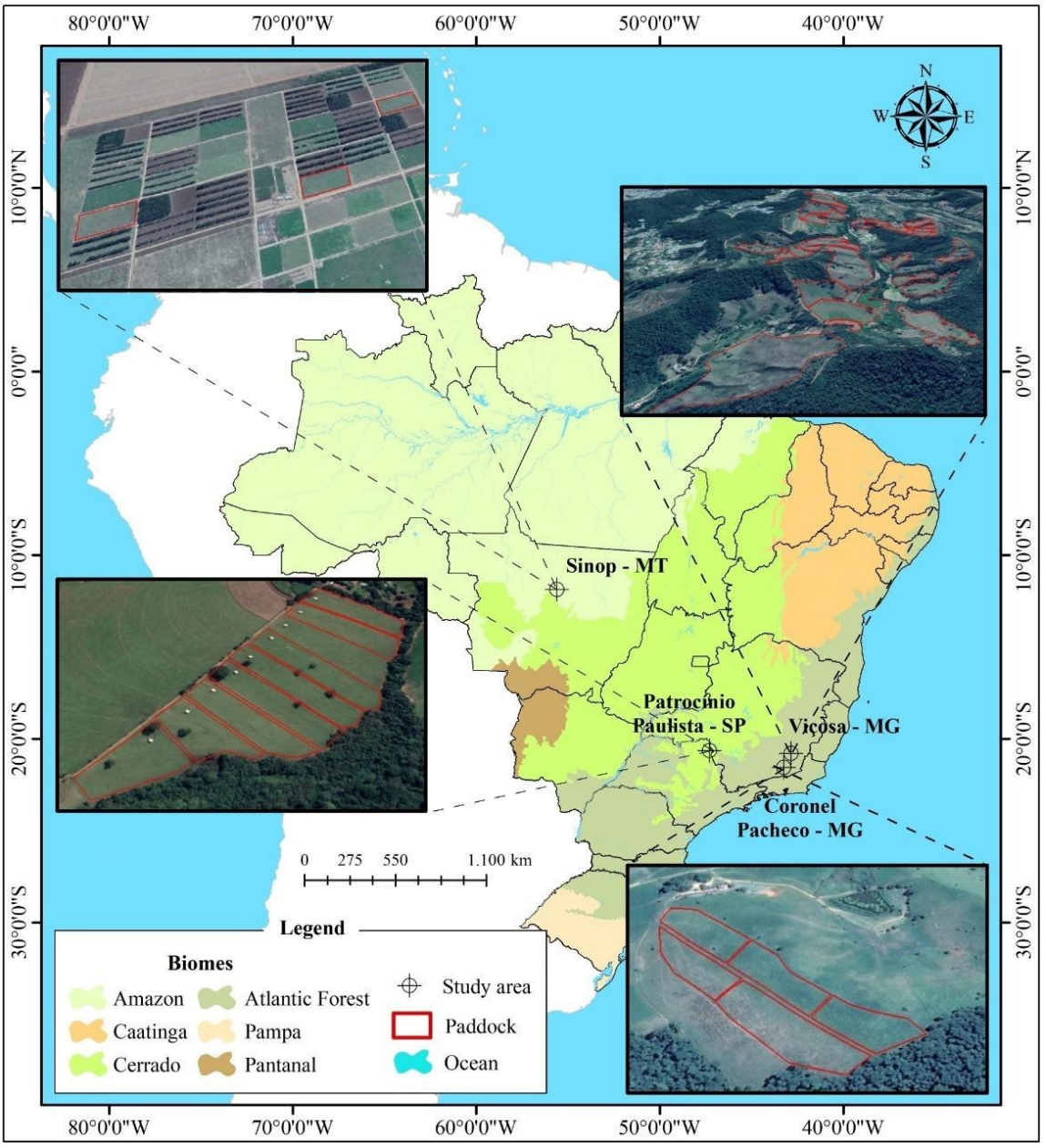

FIGURE 1 Map of Brazilian biome distribution and aboveground biomass field sampling locations

TABLE 1 Location and other information of pastures utilized for field data collection

Field ID	Location	Predominant vegetation	Relief	Biome
1	Viçosa-MG	*Brachiaria decumbens*	Mountainous	Atlantic Forest
2	Coronel Pacheco-MG	*Brachiaria decumbens/ruziziensis*	Undulating	Atlantic Forest
3	Patrocínio Paulista-SP	*Brachiaria brizantha* cv. Marandu	Flat	Cerrado
4	Sinop-MT	*Brachiaria brizantha* cv. Marandu	Flat	Amazon

2.2 | Field data collection

To quantify the pasture AGB in the field, several points were selected randomly within each paddock, and all the forage contained in the area bounded by a frame (0.25-0.64 m^2) was cut close (5cm) to the ground and packed in plastic bags. The number of sampled points varied according to the area and uniformity of the paddock, with an average of twenty points per hectare. Immediately after cutting, the sample obtained was weighed to determine the AFB, and subsequently partially dehydrated in an oven with forced air circulation at 55°C for 72h, then dried in an oven without forced air circulation at 105°C for 16h to determine the ADB and DMC in the sample. The forage biomass contained in the respective paddocks was expressed in kg ha^{-1}.

Precipitation, insolation (duration of solar brightness), and average temperature data for the sampling locations were obtained from the Meteorological Database for Teaching and Research (BDMEP) of the Instituto Nacional de Meteorologia (INMET). The rainfall, insolation and average temperature in the 10 days preceding the pasture sampling were calculated cumulatively to estimate the grass growth dynamic in response to weather conditions.

AGB data obtained in the field by cutting and weighing were used to assess the correlation between AGB and VIs, as well as with meteorological variables. Subsequently, field

data were used for calibration and validation of pasture AGB prediction models through the use of satellite imagery.

2.3 | Imagery acquisition

The satellites providing the images were Landsat-8, operated by NASA (National Aeronautics and Space Administration) with a spatial resolution of 30 m and a 16-day temporal resolution, and Sentinel-2, operated by ESA (European Space Agency) with a spatial resolution of 10 m and temporal resolution of 5 days. The only images utilized were those obtained prior to the date of biomass field data collection and with a maximum difference between data and image collection of eight days during the rainy season and twelve days during the dry period. This difference between the dates was allowed for modeling due to the period required by satellites to revisit the same location, and the recurring problem of cloud coverage in the images, ensuring a greater number of images for evaluation and observing the period of growth and morphological change of the paddock. In total, a database containing 120 observations was used for modeling. The dates of field sampling, imagery acquisition, and the corresponding dataset obtained for modeling are shown in Appendix S1. Additionally, we evaluated the relationship between VIs obtained from Landsat-8 and Sentinel-2 on the same date and paddock to ensure the interoperability between both sources.

The spectral bands of visible red (~ 665 nm) and near-infrared (~ 840 nm) referring to the selected orthorectified images were downloaded for free from the United States Geological Survey (USGS) website (Lansat-8) and ESA website (Sentinel-2) using the Semi-Automatic Classification Plugin (SCP) of the free software QGIS 3.4®. After the respective spectral bands were downloaded, they were pre-processed in the QGIS software, including reprojection of the coordinates using the DATUM WGS84 system, atmospheric correction by the dark-object subtraction (DOS1) method and radiometric correction. The atmospheric and radiometric corrections of the images were also performed using the SCP. The digital numbers of the images were converted to reflectance. From the reflectance values of the respective spectral bands, the NDVI, EVI2 (enhanced vegetation index 2), and OSAVI (optimized soil adjusted vegetation index) indices were calculated according to the equations shown in Table 2 and using the “raster calculator” tool of QGIS software.

TABLE 2 Vegetation indices calculated and respective references

Index	Equation	Reference
NDVI	(NIR-RED) / (NIR+RED)	Rouse et al. (1974)
OSAVI	(NIR-RED) / (NIR+RED+0.16)	Rondeaux et al. (1996)
EVI2	2.5*((NIR-RED) / (NIR+2.4*RED+1))	Jiang et al. (2008)

NIR: Reflectance of Near-Infrared wavelength; RED: Reflectance of Red wavelength

NDVI was chosen as it is the most commonly used index to estimate biomass of several crops, including pastures. Still, it loses sensitivity under conditions of high green biomass and the presence of exposed soil (Mutanga and Skidmore, 2004; Fern et al., 2018). Therefore, EVI2 was chosen to minimize the problem of index saturation in conditions of high biomass (Jiang et al., 2008), and OSAVI was chosen to minimize soil interference (Rondeaux et al., 1996) due to the great spatial heterogeneity of the evaluated areas.

The vector layer corresponding to the paddock was inserted into the QGIS software interface to determine the average value and standard deviation of each index within each paddock. The average index between the pixels contained in the vector was obtained using the "zonal statistics" tool. The calculated average index was then used to correlate with the data obtained in the field on dates corresponding to the date of image acquisition for later biomass prediction (Appendix S1).

2.4 | Statistical analysis

To assess the different prediction methods, the original database (n = 120) was randomly split into calibration (n = 96) and validation (n = 24) datasets. The calibration dataset was used to perform all modelling steps (pre-processing data, selection of variables, and optimization of hyperparameters). After all modeling steps, the validation dataset was applied to the final model to predict biomass.

For better model calibration, new variables were created from the combination of all variables (2x2), subtracting one from the other. All new variables created were filtered by the correlation of the new feature with the target variables. The new variable was selected to integrate the original variables if the correlation was greater than each single variable correlation.

To predict the pasture AFB, ADB, and DMC, three methods were used: SLR, using NDVI, EVI2 or OSAVI as a baseline biomass predictor (reference model), MLR with backward

elimination, starting with all variables and eliminating the highest p-value variables until all had p-values < 0.05 and RF with variable selection, removing the variables of minor importance (backward elimination) based on k-fold cross-validation (5 k-folds) performance. After variable selection, using k-fold cross-validation in the calibration dataset, the RF model hyperparameters were optimized by using the Bayesian optimization function from the *scikit-optimize library* (version 0.7.4).

The accuracy of the prediction models was then assessed by predicting the variables of interest for the validation dataset through the determination coefficient (R^2; Equation 1), and root-mean-square error (RMSE; Equation 2). All statistical analyses were run in Python 3 (version 3.7), and the flow chart of data processing and statistical analyses for biomass and DMC prediction are shown in Figure 2.

$$RR^2 = 1 - \frac{\sum_{ii=1}^{mm} (VV_{000000}^{ii} - \hat{V}_{eeoeee})^2}{\sum_{ii=1}^{mm} (VV_{000000}^{ii} - \bar{V}_{000000})^2} \quad (1)$$

in which VV_{000000}^{ii} is the observed variables, $\hat{V}_{eeoeee}$ is the model prediction, and $\bar{V}_{000000}$ is the average of the observed variables.

$$RRMMMMEE = \sqrt{\frac{1}{mm}\sum_{ii=1}^{mm}(\hat{V}_{eeoeee} - VV_{000000}^{ii})^2} \quad (2)$$

in which mm is the number of observed variables.

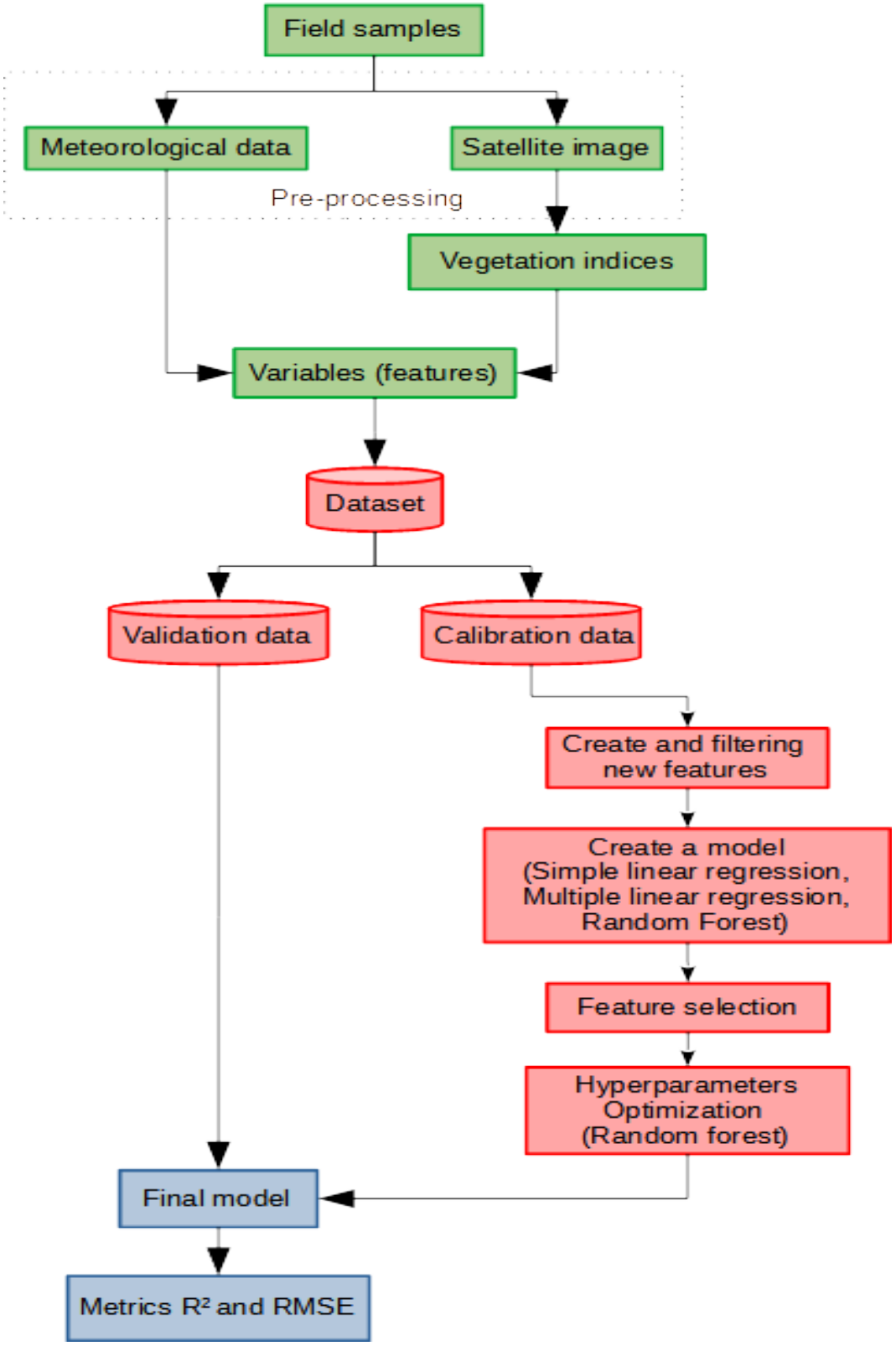

FIGURE 2 Flow chart of data processing and statistical analyses for biomass and dry matter concentration prediction

3 | RESULTS

3.1 | Correlation between variables

Significant correlations were found between most of the variables analyzed, including, notably, a strong positive correlation between VIs and AFB, and negative between VIs and DMC (Figure 3). Among the VIs, EVI2 had the lowest correlation coefficient, although significant, with AFB (r = 0.74) and DMC (r = 0.77), while NDVI and OSAVI showed a stronger and similar correlation (r > 0.82). Among the meteorological variables, the accumulated average temperature of the period presented the weakest correlation with AFB (r = 0.44) and DMC (r = 0.47), while the accumulated rainfall and insolation moderately correlated with pasture variables (r > 0.55). Both VIs and meteorological variables were better correlated with AFB and DMC than ADB, although all correlations were significant.

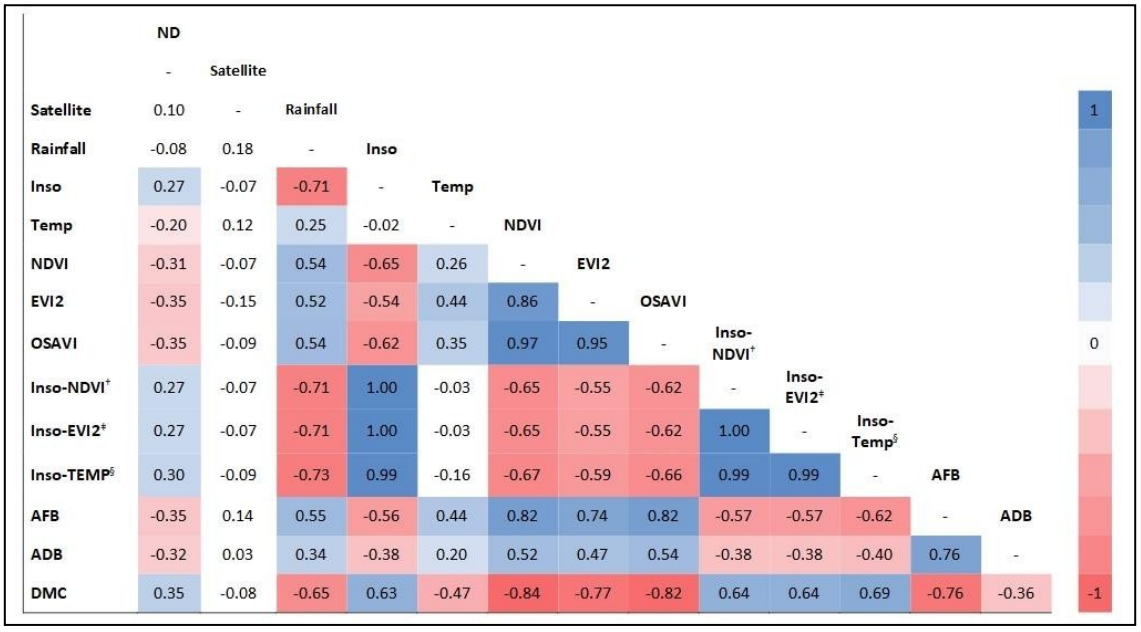

	ND	Satellite	Rainfall	Inso	Temp	NDVI	EVI2	OSAVI	Inso-NDVI†	Inso-EVI2‡	Inso-Temp§	AFB	ADB
Satellite	0.10	-											
Rainfall	-0.08	0.18	-										
Inso	0.27	-0.07	-0.71	-									
Temp	-0.20	0.12	0.25	-0.02	-								
NDVI	-0.31	-0.07	0.54	-0.65	0.26	-							
EVI2	-0.35	-0.15	0.52	-0.54	0.44	0.86	-						
OSAVI	-0.35	-0.09	0.54	-0.62	0.35	0.97	0.95	-					
Inso-NDVI†	0.27	-0.07	-0.71	1.00	-0.03	-0.65	-0.55	-0.62	-				
Inso-EVI2‡	0.27	-0.07	-0.71	1.00	-0.03	-0.65	-0.55	-0.62	1.00	-			
Inso-TEMP§	0.30	-0.09	-0.73	0.99	-0.16	-0.67	-0.59	-0.66	0.99	0.99	-		
AFB	-0.35	0.14	0.55	-0.56	0.44	0.82	0.74	0.82	-0.57	-0.57	-0.62	-	
ADB	-0.32	0.03	0.34	-0.38	0.20	0.52	0.47	0.54	-0.38	-0.38	-0.40	0.76	-
DMC	0.35	-0.08	-0.65	0.63	-0.47	-0.84	-0.77	-0.82	0.64	0.64	0.69	-0.76	-0.36

FIGURE 3 Pearson correlation map of variables. ND: number of days between image acquisition and field sampling dates; Satellite: sensor type used for acquire images; Inso: insolation; Temp: temperature; †combination between insolation and NDVI; ‡combination between insolation and EVI2; §combination between insolation and temperature; AFB: aboveground fresh biomass; ADB: aboveground dry biomass; DMC: dry matter concentration. All coloured correlations are significant by test t ($p < 0.05$).

The satellite used for image acquisition (Landsat-8 or Sentinel-2) was not significantly correlated with any other variable (Figure 3), and the VIs obtained from both image sources showed a strong correlation, with R^2 values ranging from 0.82 to 0.92 (Figure 4).

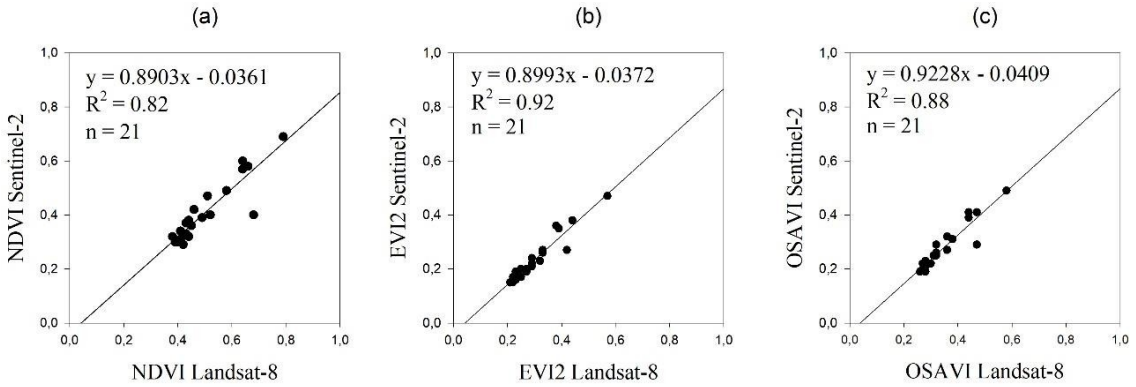

FIGURE 4 Relationship between (a) NDVI, (b) EVI2 and (c) OSAVI values obtained with Landsat-8 and Sentinel-2 images on the same date and paddock.

3.2 | Prediction models results

The prediction of AFB and DMC based on the SLR using different VIs (NDVI, EVI2 or OSAVI) as predictor variable demonstrated good accuracy, although lower than that of other methods, with R^2 and RMSE for the validation data ranging from 0.72 to 0.73 and 4241 to 4272 kg ha^{-1} respectively, for AFB prediction (Table 3). For DMC prediction the R^2 ranged from 0.70 to 0.73 and RMSE ranged from 10 to 11% (Table 3). The difference in performance between the predictor variables was negligible. The models for AFB and DMC prediction by SLR are shown in Table 3.

TABLE 3 Simple Linear Regression analysis for aboveground fresh biomass (AFB) and dry matter concentration (DMC) prediction

Predictor variable	Model	R^2	RMSE
	AFB prediction (kg ha^{-1})		
NDVI	y = 42340 NDVI - 10450	0.73	4241,1
EVI2	y = 34860 EVI2	0.72	4248,3
OSAVI	y = 53220 OSAVI - 8081.8025	0.73	4272,4
	DMC prediction (%)		
NDVI	y = -88.8984 NDVI + 92.3287	0.70	11
EVI2	y = -82.8979 EVI2 + 75.0537	0.72	11
OSAVI	y = -108.9412 OSAVI + 86.2398	0.73	10

MLR demonstrated intermediate predictive performance compared to other methods. After backward selection, the variables selected for the prediction of AFB were the type of satellite used for image acquisition, OSAVI index, and the combinations between temperature x insolation, EVI2 x insolation, and NDVI x insolation. The R^2 and RMSE for the MLR model for prediction of validation data were 0.76 and 3976.1 kg ha^{-1}, respectively, and 0.78 and 9.5%, respectively, for AFB and DMC prediction (Figure 5). The models for AFB and DMC prediction by MLR are shown in equations (4) and (5).

$$AAFFBB = -24850 + 3128.0386\ MMSSeeeeTTiiiiii + 45120\ OOMMAAVVII - 803.3964\ IInnoooo_{TTeemmpp} + 14690\ IInnoooo_{EEVVII2} - 13940\ IInnoooo_{NNNNVVII} \quad (4)$$

in which $MMSSeeeeSSSSiieeee$ represents a value assigned to the sensor type used for acquire images, $IInnoooo_{TTeemmpp}$ is the combination between insolation and temperature, $IInnoooo_{EEVVII2}$ is the combination between insolation and EVI2, and $IInnoooo_{NNNNVVII}$ is the combination between insolation and NDVI.

$$NNMMDD = 124.7337 + 0.6512\ nnnn - 0.0733\ RRSSiinnRRSSSSSS - 48.7546\ IInnooooSSSSeeiioonn - 25.4040\ TTeemmppeeTTSSeeTTTTee - 120.9216\ NNNNVVII - 64.8467\ EEVVII2 + 239.9650\ OOMMAAVVII - 23.3506\ IInnoooo_{TTeemmpp} + 72.1669\ IInnoooo_{NNNNVVII} \quad (5)$$

in which *nnnn* is the number of days between image acquisition date and field sampling date and *Rainfall*, *Insolation* and *Temperature* represents the respective values accumulated in ten days.

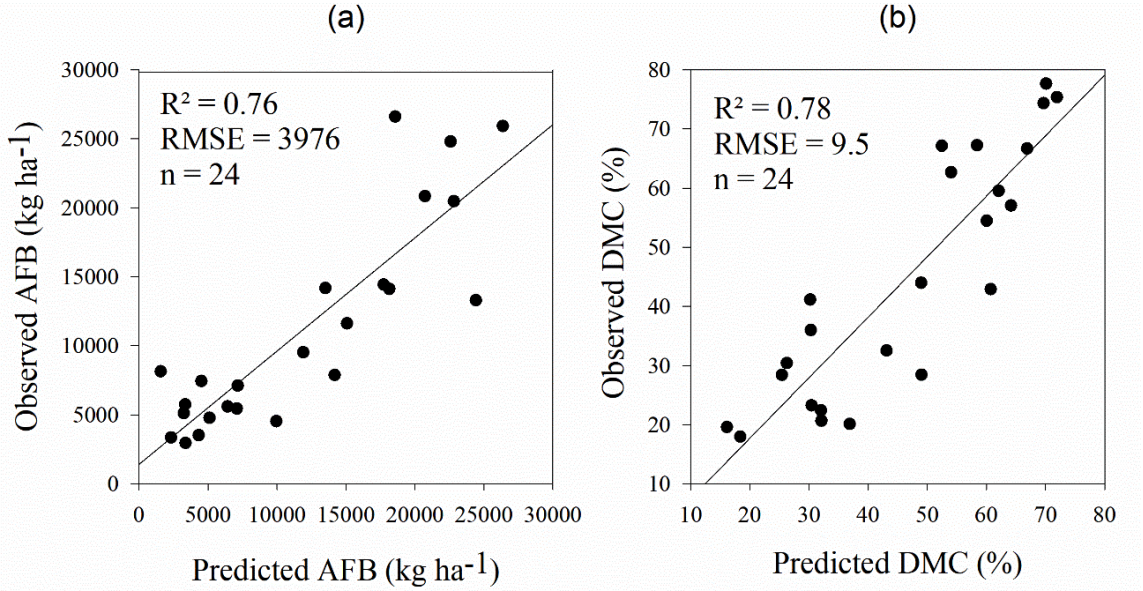

FIGURE 5 Prediction by multiple linear regression for (a) aboveground fresh biomass (AFB) and (b) dry matter concentration (DMC)

The best prediction performance of pasture AFB and DMC was achieved with the RF algorithm. During the modeling, the most important attributes selected for the construction of the RF model for prediction of AFB and DMC were NDVI, EVI2, OSAVI, accumulated precipitation, and average accumulated temperature, with emphasis on the importance value attributed to the VIs (Figure 6).

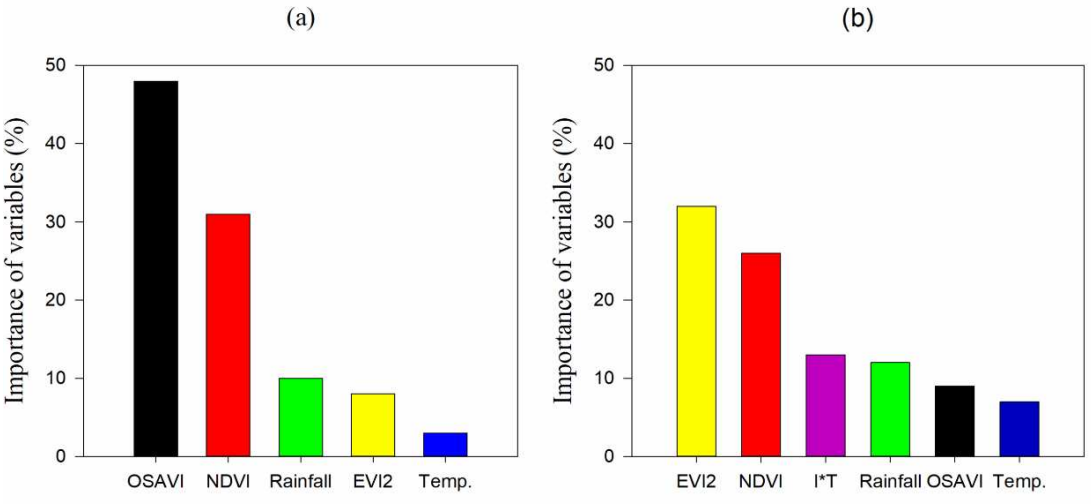

FIGURE 6 Importance of variables attributed by the random forest algorithm for (a) aboveground fresh biomass (AFB) and (b) dry matter concentration (DMC) prediction. Temp.: Temperature; I*T: Combination between insolation and temperature

The RF algorithm R^2 and RMSE were 0.85 and 2947.1 kg ha^{-1}, respectively, and 0.85 and 7.9% for AFB and DMC prediction, respectively, for the validation data (Figure 7).

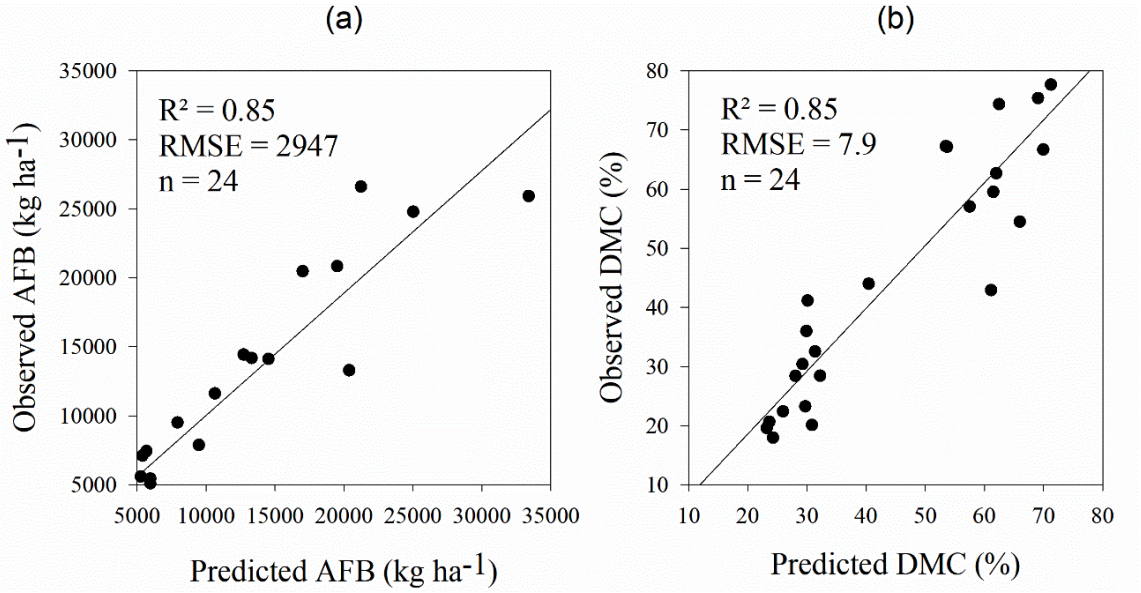

FIGURE 7 Prediction by random forest algorithm for (a) aboveground fresh biomass (AFB) and (b) dry matter concentration (DMC)

Despite the significant correlations between the main predictor variables and ADB, none of the three methods were efficient in predicting ADB, with R^2 values ranging from 0.19 to

0.35 (Figure 8). We chose to represent only the NDVI index in figure 8 because both VIs performed similarly and it is the VI most widely used for estimates of vegetation cover.

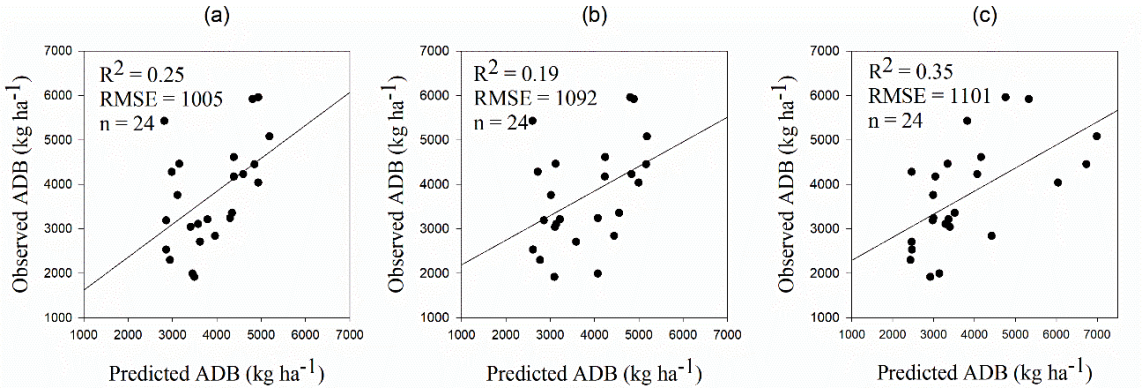

FIGURE 8 Aboveground dry biomass (ADB) prediction using (a) simple linear regression with NDVI, (b) multiple linear regression, and (c) random forest algorithm

4 | DISCUSSION

The results of our study are consistent with several other studies in demonstrating a strong correlation between VIs obtained by RS through satellites and pasture biomass. Edirisinghe et al. (2012) found a strong positive correlation (r = 0.81) between pasture biomass and NDVI in a study conducted in New Zealand. Barrachina et al. (2015) also found a strong correlation (R^2 = 0.82) between the biomass of mountain pastures and the EVI and NDVI index. In contrast, Ferreira et al. (2013) found weaker, but significant correlations between green biomass and NDVI (r = 0.65) or EVI (r = 0.62), while Fern et al. (2018) demonstrated that in areas with scarce vegetation or the presence of exposed soil patches, the OSAVI index may be more suitable for estimating green biomass because it minimizes the variability caused by soil reflectance. This index is appropriate for use in the present study since tropical pasture areas present considerable spatial variability in terms of grass coverage and, consequently, percentage of exposed soil. Consistent with the present study, Guerini Filho et al. (2020) conducted a study in Brazil and found a strong correlation between different VIs obtained via the Sentinel-2 satellite and pasture biomass, demonstrating that it is possible to use spectral information obtained through the Multi Spectral Instrument (MSI) sensor to predict pasture biomass in Brazil.

The significant correlations between biomass and meteorological data demonstrate the importance of rainfall, insolation, and temperature data in the prediction of pasture biomass in

our study. According to Xu et al. (2018), precipitation, temperature, and the interaction between precipitation and temperature explain 65.5, 14.5, and 9.8%, respectively, of the variation in the LAI of pastures. Studies by Hill et al. (2004) and Donald et al. (2010) also demonstrated that climatic data, combined with VIs obtained by RS, allow for accurate prediction of the growth rate of the pasture, and can play an important role in the prediction of biomass. Similarly, Fontana et al. (2018), working on natural pastures in a subtropical climate in Brazil, recommended the combination of meteorological data and spectral indexes to adjust forage accumulation models.

Strong correlations were identified between VIs obtained by the different satellites. Chakhar et al. (2020) used Landsat-8 and Sentinel-2 images for crop classification and identified that there is strong correlation between IVs obtained by both image sources and that the linear calibration of the VIs does not contribute to improve crop classification, demonstrating the interoperability between satellites. No significant correlations were identified between the satellite used for image acquisition (Landsat-8 or Sentinel-2) and any variable of interest. In addition, the importance value attributed by the RF algorithm to the type of sensor used was negligible, suggesting that both sensors (Operational Land Imager and MSI) can be used in the prediction of *Brachiaria* (syn. *Urochloa*) pasture biomass in Brazil. Wang et al. (2019) also demonstrated the potential of integrating Sentinel-2 and Landsat-8 imagery into monitoring of the seasonal dynamic of grasslands, consistent with our study.

We conducted a SLR analysis between the variables of interest (AFB, ADB, and DMC) predicted by VIs (NDVI, EVI2 or OSAVI) and variables measured in the field to use as a reference in our study, as it is the simplest method (baseline) for predicting such variables. Goswami et al. (2015) reported a strong exponential relationship between NDVI and biomass ($R^2 = 0.70$) for six different species in Canada and indicated saturation of the index at biomasses above 100 g m^{-2}. Similarly, Pezzopane et al. (2019), using VIs to monitor pastures formed by grasses of the genus *Brachiaria* (syn. *Urochloa*), found a strong exponential relationship between NDVI and LAI, as well as between NDVI and leaf biomass for different systems. We identified a strong linear relationship between the variables estimated through the VIs and measured in the field (Table 3), suggesting that there was no index saturation effect in the present study.

The present study demonstrates that the RF algorithm is more accurate than MLR for predicting pasture biomass in Brazil. Consistent with our study, Mutanga et al. (2012) also compared the performance of the RF with that of the stepwise MLR in the prediction of pasture

biomass and found a higher accuracy with the RF algorithm. Wang et al. (2017) also used meteorological data and images from two different satellites to predict pasture biomass in China using different prediction algorithms and determined the RF algorithm was superior to the others. Similarly, Wu et al. (2016) and Li et al. (2017) indicated that the RF algorithm associated with Landsat imagery provided accurate estimates of AGB and grasslands LAI. Otgonbayar et al. (2019) used VIs calculated from Landsat-8 imagery to develop pasture biomass prediction models and found the RF algorithm demonstrated good predictive performance (R^2 = 0.76; RMSE = 98 kg ha^{-1}). The estimated error for biomass prediction in the present study was well above the reported by Otgonbayar et al. (2019); however these authors collected data in an arid climate, with low temperatures and precipitation, and studied forages with a lower production potential (mean biomass value of 257 kg DM ha^{-1}) than the tropical grasses evaluated in our study, of which the average biomass was 12978 kg FB ha^{-1} and 3890 kg DM ha^{-1} during the evaluated years. Considering the pasture biomass measured in the two studies, our RMSE was approximately 23% and 28% of the average AFB and ADB measured, respectively, while Otgonbayar et al. (2019), using RF for prediction, obtained an RMSE of approximately 38% of the average ADB observed. Pezzopane et al. (2019) analyzed data from climatic conditions similar to ours, with tropical grasses of the genus *Brachiaria* (syn. *Urochloa*) in Brazil, and used NDVI to estimate forage biomass in two different production systems. The RMSE for the total biomass estimates were 961 kg DM ha^{-1}, approximately 30% of the average biomass observed (3134 kg DM ha^{-1}). Cisneros et al. (2020) also estimated the biomass productivity of several tropical grasses and showed R^2 = 0.54 and RMSE = 1800 kg ha^{-1} for estimates. In contrast, Mutanga et al. (2012) estimated the RMSE of the prediction of pasture biomass in South Africa was approximately 13% of the average biomass observed, while Mundava et al. (2014) observed that better estimates of VI-based biomass were obtained when the areas were grouped in terms of similar botanical composition than estimates combining different forages. This observation demonstrates the need for further development of specific prediction models for each location and type of predominant forage.

None of the three methods was efficient in predicting ADB. This result was not expected, but it can be explained by the lower variability in ADB data in the database used (a minimum of 1129 kg ha^{-1} and a maximum of 9080 kg ha^{-1}), while the variability of the AFB data was much greater (2320 to 42240 kg ha^{-1}), which may have reduced the R^2 of the ADB prediction models and increased the RMSE of the AFB prediction models. This small variation in ADB data relative to the variation in AFB can be explained by the seasonal variation in the

structural composition of the pasture, and consequently, in the DMC. During the rainy months of the years 2015 to 2019, the average DMC was 26.2%, while the average DMC for the dry months was 63.3% (Appendix S1). Thus, during the pasture growing season, we had a substantial increase in the AFB of the pasture, leading to an increase in the VIs obtained in this period, which was not accompanied by a proportional increase in ADB due to the reduced DMC in the period. Likewise, during dry periods, the reduction in AFB and VIs was not accompanied by a proportional reduction in ADB due to the high DMC of the pasture. The high DMC of the grasses during the dry period may have resulted from modifications in the plant morphological composition due to changes in climatic conditions and the consequent increase in senescent material. Pezzopane et al. (2019) reported poorer VIs performance in estimating total forage biomass than estimating leaf mass and explained this observation by differences in structural composition and the senescent material proportion between different areas. Similarly, Tong et al. (2019) used MLR model for estimating AFB and ADB at two locations and also observed better predictive performance for AFB compared to ADB. Mundava et al. (2014) in a previous study tested the relationship between VIs obtained by Landsat (ETM +) imagery and biomass from different pasture areas in Australia and also found better relationships between VIs and green biomass than dry biomass.

Despite this, AFB can be used to characterize herbage mass of a grassland and the high prediction accuracy of AFB and DMC identified in our study indicates that it is possible to quantify the forage biomass using the AFB and DMC to assess the ADB, thereby assisting the grazing management of tropical grasses in Brazil. Notably, our study was conducted in pastures in different regions of Brazil, with high heterogeneity of climate, relief, and soil and high spatial variability of species, typical of our pasturelands, indicating that the RF model can be used to quantify biomass on the Brazilian *Brachiaria* (syn. *Urochloa*) pastures.

5 | CONCLUSIONS

The NDVI, EVI2, and OSAVI indices strongly correlated with biomass and DMC of *Brachiaria* (syn. *Urochloa*) pastures and can be used as a tool for monitoring tropical grasslands in Brazil.

The MLR and RF algorithms improved the accuracy of biomass prediction using both Landsat-8 and Sentinel-2 imagery, combined with meteorological data to assess AFB and DMC of *Brachiaria* (syn. *Urochloa*) pastures in Brazil. Further research on tropical grasses is needed

to evaluate different VIs, as well as other machine learning techniques, to improve the accuracy of prediction of ADB and to support pasture management in Brazil.

REFERENCES

Ali, I., Greifeneder, F., Stamenkovic, J., Neumann, M., & Notarnicola, C. (2015). Review of Machine Learning Approaches for Biomass and Soil Moisture Retrievals from Remote Sensing Data. *Remote Sensing*, *7*(12), 16398–16421. https://doi.org/10.3390/rs71215841

Barbero, R. P., Malheiros, E. B., Araújo, T. L. R., Nave, R. L. G., Mulliniks, J. T., Berchielli, T. T., … Reis, R. A. (2015). Combining Marandu grass grazing height and supplementation level to optimize growth and productivity of yearling bulls. *Animal Feed Science and Technology*, *209*, 110–118. https://doi.org/10.1016/j.anifeedsci.2015.09.010

Barrachina, M., Cristóbal, J., & Tulla, A. F. (2015). Estimating above-ground biomass on mountain meadows and pastures through remote sensing. *International Journal of Applied Earth Observation and Geoinformation*, *38*, 184–192. https://doi.org/10.1016/j.jag.2014.12.002

Batistoti, J., Marcato Junior, J., Ítavo, L., Matsubara, E., Gomes, E., Oliveira, B., … Dias, A. (2019). Estimating Pasture Biomass and Canopy Height in Brazilian Savanna Using UAV Photogrammetry. *Remote Sensing*, *11*(20), 2447. https://doi.org/10.3390/rs11202447

Carnevalli, R. A., Silva, S. C. D., Bueno, A. A. O., Uebele, M. C., Bueno, F. O., Hodgson, J., … Morais, J. P. G. (2006). Herbage production and grazing losses in Panicum maximum cv. Mombaça under four grazing managements. *Tropical Grasslands,* 40, 165-176.

Chakhar, A., Ortega-Terol, D., Hernández-López, D., Ballesteros, R., Ortega, J. F., & Moreno, M. A. (2020). Assessing the Accuracy of Multiple Classification Algorithms for Crop Classification Using Landsat-8 and Sentinel-2 Data. *Remote Sensing*, *12*(11), 1735. https://doi.org/10.3390/rs12111735

Cisneros, A., Fiorio, P., Menezes, P., Pasqualotto, N., Van Wittenberghe, S., Bayma, G., & Furlan Nogueira, S. (2020). Mapping Productivity and Essential Biophysical Parameters of Cultivated Tropical Grasslands from Sentinel-2 Imagery. *Agronomy*, *10*(5), 711. https://doi.org/10.3390/agronomy10050711

de Oliveira, O. C., de Oliveira, I. P., Alves, B. J. R., Urquiaga, S., & Boddey, R. M. (2004). Chemical and biological indicators of decline/degradation of Brachiaria pastures in the Brazilian Cerrado. *Agriculture, Ecosystems & Environment*, *103*(2), 289–300. https://doi.org/10.1016/j.agee.2003.12.004

Delevatti, L. M., Cardoso, A. S., Barbero, R. P., Leite, R. G., Romanzini, E. P., Ruggieri, A. C., & Reis, R. A. (2019). Effect of nitrogen application rate on yield, forage quality, and animal performance in a tropical pasture. *Scientific Reports*, *9*(1), 7596. https://doi.org/10.1038/s41598-019-44138-x

Donald, G. E., Gherardi, S. G., Edirisinghe, A., Gittins, S. P., Henry, D. A., & Mata, G. (2010). Using MODIS imagery, climate and soil data to estimate pasture growth rates on farms in the south-west of Western Australia. *Animal Production Science*, *50*(6), 611. https://doi.org/10.1071/AN09159

Edirisinghe, A., Clark, D., & Waugh, D. (2012). Spatio-temporal modelling of biomass of intensively grazed perennial dairy pastures using multispectral remote sensing. *International Journal of Applied Earth Observation and Geoinformation*, *16*, 5–16. https://doi.org/10.1016/j.jag.2011.11.006

Fern, R. R., Foxley, E. A., Bruno, A., & Morrison, M. L. (2018). Suitability of NDVI and OSAVI as estimators of green biomass and coverage in a semi-arid rangeland. *Ecological Indicators*, *94*, 16–21. https://doi.org/10.1016/j.ecolind.2018.06.029

Ferreira, L., Fernandez, L., Sano, E., Field, C., Sousa, S., Arantes, A., & Araújo, F. (2013). Biophysical Properties of Cultivated Pastures in the Brazilian Savanna Biome: An Analysis in the Spatial-Temporal Domains Based on Ground and Satellite Data. *Remote Sensing*, *5*(1), 307–326. https://doi.org/10.3390/rs5010307

Fontana, D. C., Junges, A. H., Bremm, C., Schaparini, L. P., Mengue, V. P., Wagner, A. P. L., & Carvalho, P. (2018). NDVI and meteorological data as indicators of the Pampa biome natural grasslands growth. *Bragantia*, *77*(2), 404–414. https://doi.org/10.1590/1678-4499.2017222

Gitelson, A. & Merzlyak, M. N. (1994) Quantitative Estimation of Chlorophyll-a using Reflectance Spectra: Experiments with Autumn Chestnut and Maple Leaves. 6. J. *Photochemistry and Photobiology B: Biology*, 22, 247-252.

Goswami, S., Gamon, J., Vargas, S., & Tweedie, C. (2015). *Relationships of NDVI, Biomass, and Leaf Area Index (LAI) for six key plant species in Barrow, Alaska* [Preprint]. PeerJ PrePrints. https://doi.org/10.7287/peerj.preprints.913v1

Gu, Y., Wylie, B. K., Howard, D. M., Phuyal, K. P., & Ji, L. (2013). NDVI saturation adjustment: A new approach for improving cropland performance estimates in the Greater Platte River Basin, USA. *Ecological Indicators*, *30*, 1–6. https://doi.org/10.1016/j.ecolind.2013.01.041

Guerini Filho, M., Kuplich, T. M., & Quadros, F. L. F. D. (2020). Estimating natural grassland biomass by vegetation indices using Sentinel 2 remote sensing data. *International Journal of Remote Sensing*, *41*(8), 2861–2876. https://doi.org/10.1080/01431161.2019.1697004

Hill, M. J., Donald, G. E., Hyder, M. W., & Smith, R. C. G. (2004). Estimation of pasture growth rate in the south west of Western Australia from AVHRR NDVI and climate data. *Remote Sensing of Environment*, *93*(4), 528–545. https://doi.org/10.1016/j.rse.2004.08.006

Hill, M. J., Zhou, Q., Sun, Q., Schaaf, C. B., & Palace, M. (2017). Relationships between vegetation indices, fractional cover retrievals and the structure and composition of Brazilian Cerrado natural vegetation. *International Journal of Remote Sensing*, *38*(3), 874–905. https://doi.org/10.1080/01431161.2016.1271959

Idowu, S., Saguna, S., Åhlund, C., & Schelén, O. (2016). Applied machine learning: Forecasting heat load in district heating system. *Energy and Buildings*, *133*, 478–488. https://doi.org/10.1016/j.enbuild.2016.09.068

Instituto Brasileiro de Geografia e Estatística (IBGE). (2017). Censo Agropecuário. Retrieved from: https://biblioteca.ibge.gov.br/index.php/biblioteca-catalogo?view=detalhes&id=73096 (accessed on 27 May 2020).

Insua, J. R., Utsumi, S. A., & Basso, B. (2019). Estimation of spatial and temporal variability of pasture growth and digestibility in grazing rotations coupling unmanned aerial vehicle (UAV) with crop simulation models. *PLOS ONE*, *14*(3), e0212773. https://doi.org/10.1371/journal.pone.0212773

Jank, L., Barrios, S. C., do Valle, C. B., Simeão, R. M., & Alves, G. F. (2014). The value of improved pastures to Brazilian beef production. *Crop and Pasture Science*, *65*(11), 1132. https://doi.org/10.1071/CP13319

Jiang, Z., Huete, A., Didan, K., & Miura, T. (2008). Development of a two-band enhanced vegetation index without a blue band. *Remote Sensing of Environment*, *112*(10), 3833–3845. https://doi.org/10.1016/j.rse.2008.06.006

Li, Zhen-wang, Xin, X., Tang, H., Yang, F., Chen, B., & Zhang, B. (2017). Estimating grassland LAI using the Random Forests approach and Landsat imagery in the meadow steppe

of Hulunber, China. *Journal of Integrative Agriculture*, *16*(2), 286–297. https://doi.org/10.1016/S2095-3119(15)61303-X

Li, Zhiguo, Han, G., Zhao, M., Wang, J., Wang, Z., Kemp, D. R., … Langford, C. (2015). Identifying management strategies to improve sustainability and household income for herders on the desert steppe in Inner Mongolia, China. *Agricultural Systems*, *132*, 62–72. https://doi.org/10.1016/j.agsy.2014.08.011

Liu, H. Q. & Huete, A. (1995). A Feedback Based Modification of the NDVI to Minimize Canopy Background and Atmospheric Noise. *IEEE Transactions on Geoscience and Remote Sensing*.

Lussem, U., Bolten, A., Menne, J., Gnyp, M. L., Schellberg, J., & Bareth, G. (2019). Estimating biomass in temperate grassland with high resolution canopy surface models from UAV-based RGB images and vegetation indices. *Journal of Applied Remote Sensing*, *13*(03), 1. https://doi.org/10.1117/1.JRS.13.034525

Machado, V. D., Fonseca, D. M., Lima, M. A., Martuscello, J. A., Paciullo, D. S. C., & Chizzotti, F. H. M. (2020). Grazing management strategies for *Urochloa decumbens* (Stapf) R. Webster in a silvopastoral system under rotational stocking. *Grass and Forage Science*, gfs.12491. https://doi.org/10.1111/gfs.12491

Mandanici, E., & Bitelli, G. (2016). Preliminary Comparison of Sentinel-2 and Landsat 8 Imagery for a Combined Use. *Remote Sensing*, *8*(12), 1014. https://doi.org/10.3390/rs8121014

Michez, A., Lejeune, P., Bauwens, S., Herinaina, A., Blaise, Y., Castro Muñoz, E., … Bindelle, J. (2019). Mapping and Monitoring of Biomass and Grazing in Pasture with an Unmanned Aerial System. *Remote Sensing*, *11*(5), 473. https://doi.org/10.3390/rs11050473

Mundava, C., Helmholz, P., Schut, A. G. T., Corner, R., McAtee, B., & Lamb, D. W. (2014). Evaluation of vegetation indices for rangeland biomass estimation in the Kimberley area of Western Australia. *ISPRS Annals of Photogrammetry, Remote Sensing and Spatial Information Sciences*, *II–7*, 47–53. https://doi.org/10.5194/isprsannals-II-7-47-2014

Mutanga, O., & Skidmore, A. K. (2004). Narrow band vegetation indices overcome the saturation problem in biomass estimation. *International Journal of Remote Sensing*, *25*(19), 3999–4014. https://doi.org/10.1080/01431160310001654923

Mutanga, O., Adam, E., & Cho, M. A. (2012). High density biomass estimation for wetland vegetation using WorldView-2 imagery and random forest regression algorithm. *International Journal of Applied Earth Observation and Geoinformation*, *18*, 399–406. https://doi.org/10.1016/j.jag.2012.03.012

Otgonbayar, M., Atzberger, C., Chambers, J., & Damdinsuren, A. (2019). Mapping pasture biomass in Mongolia using Partial Least Squares, Random Forest regression and Landsat 8 imagery. *International Journal of Remote Sensing*, *40*(8), 3204–3226. https://doi.org/10.1080/01431161.2018.1541110

Punalekar, S. M., Verhoef, A., Quaife, T. L., Humphries, D., Bermingham, L., & Reynolds, C. K. (2018). Application of Sentinel-2A data for pasture biomass monitoring using a physically based radiative transfer model. *Remote Sensing of Environment*, *218*, 207–220. https://doi.org/10.1016/j.rse.2018.09.028

Rondeaux, G., Steven, M., & Baret, F. (1996). Optimization of soil-adjusted vegetation indices. *Remote Sensing of Environment*, *55*(2), 95–107. https://doi.org/10.1016/0034-4257(95)00186-7

Rouse, W. J., Haas, R. H., Schell, J. A., Deering, D. W. (1974). Monitoring vegetation systems in the great plains with ERTS. Retrieved from: https://ntrs.nasa.gov/search.jsp?R=19740022614 (accessed on 27 May 2020).

Sanderson, M. A., Rotz, C. A., Fultz, S. W., & Rayburn, E. B. (2001). Estimating Forage Mass with a Commercial Capacitance Meter, Rising Plate Meter, and Pasture Ruler. *Agronomy Journal*, *93*(6), 1281–1286. https://doi.org/10.2134/agronj2001.1281

Santana, S. S., Brito, L. F., Azenha, M. V., Oliveira, A. A., Malheiros, E. B., Ruggieri, A. C., & Reis, R. A. (2017). Canopy characteristics and tillering dynamics of Marandu palisade grass pastures in the rainy-dry transition season. *Grass and Forage Science*, *72*(2), 261–270. https://doi.org/10.1111/gfs.12234

Santos, M. E. R., Fonseca, D. M. da, Gomes, V. M., Pimentel, R. M., Albino, R. L., & Silva, S. P. da. (2013). Signal grass structure at different sites of the same pasture under three grazing intensities. *Acta Scientiarum. Animal Sciences*, *35*(1), 73–78. https://doi.org/10.4025/actascianimsci.v35i1.11801

Terra, S., de Andrade Gimenes, F. M., Giacomini, A. A., Gerdes, L., Manço, M. X., de Mattos, W. T., & Batista, K. (2020). Seasonal alteration in sward height of Marandu palisade grass (Brachiaria brizantha) pastures managed by continuous grazing interferes with forage production. *Crop and Pasture Science*, *71*(3), 285. https://doi.org/10.1071/CP19156

Tong, X., Duan, L., Liu, T., & Singh, V. P. (2019). Combined use of in situ hyperspectral vegetation indices for estimating pasture biomass at peak productive period for harvest decision. *Precision Agriculture*, *20*(3), 477–495. https://doi.org/10.1007/s11119-018-9592-3

Wang, J., Xiao, X., Bajgain, R., Starks, P., Steiner, J., Doughty, R. B., & Chang, Q. (2019). Estimating leaf area index and aboveground biomass of grazing pastures using Sentinel-1, Sentinel-2 and Landsat images. *ISPRS Journal of Photogrammetry and Remote Sensing*, *154*, 189–201. https://doi.org/10.1016/j.isprsjprs.2019.06.007

Wang, Y., Wu, G., Deng, L., Tang, Z., Wang, K., Sun, W., & Shangguan, Z. (2017). Prediction of aboveground grassland biomass on the Loess Plateau, China, using a random forest algorithm. *Scientific Reports*, *7*(1), 6940. https://doi.org/10.1038/s41598-017-07197-6

Wijesingha, J., Astor, T., Schulze-Brüninghoff, D., Wengert, M., & Wachendorf, M. (2020). Predicting Forage Quality of Grasslands Using UAV-Borne Imaging Spectroscopy. *Remote Sensing*, *12*(1), 126. https://doi.org/10.3390/rs12010126

Wu, C., Shen, H., Shen, A., Deng, J., Gan, M., Zhu, J., … Wang, K. (2016). Comparison of machine-learning methods for above-ground biomass estimation based on Landsat imagery. *Journal of Applied Remote Sensing*, *10*(3), 035010. https://doi.org/10.1117/1.JRS.10.035010

Xu, D., Chen, B., Yan, R., Yan, Y., Sun, X., Xu, L., & Xin, X. (2019). Quantitative monitoring of grazing intensity in the temperate meadow steppe based on remote sensing data. *International Journal of Remote Sensing*, *40*(5–6), 2227–2242. https://doi.org/10.1080/01431161.2018.150073

Supporting information

Appendix S1 – Field sampling date, image acquisition date and modeling dataset. For all indexes mean and standard deviation (SD) are presented

Field ID	Image date	Field sampling	Satellite	Rainfall (mm)	Insolation (hours)	Average temperature (°C)	AFB (kg ha^{-1})	ADB (kg ha^{-1})	DMC (%)	NDVI		EVI2		OSAVI	
										Mean	SD	Mean	SD	Mean	SD
Calibration dataset															
4	11/11/2015	11/12/2015	Landsat-8	52.9	74.9	26.71	9471	3202	33.81	0.48	0.05	0.49	0.06	0.41	0.04
4	11/11/2015	11/12/2015	Landsat-8	52.9	74.9	26.71	4532	1993	43.97	0.44	0.04	0.44	0.04	0.38	0.03
4	12/4/2015	12/8/2015	Landsat-8	71.4	72.0	27.34	8053	2991	37.15	0.49	0.07	0.80	0.13	0.47	0.07
4	12/4/2015	12/8/2015	Landsat-8	71.4	72.0	27.34	7419	2674	36.04	0.48	0.03	0.78	0.05	0.46	0.03
4	12/4/2015	12/8/2015	Landsat-8	71.4	72.0	27.34	9331	2949	31.61	0.51	0.03	0.83	0.07	0.49	0.03
2	12/14/2015	12/22/2015	Landsat-8	181.4	40.6	22.24	7882	3242	41.13	0.64	0.04	0.39	0.05	0.44	0.04
4	4/3/2016	4/5/2016	Landsat-8	33.9	49.7	26.43	14432	3359	23.27	0.65	0.06	0.45	0.05	0.47	0.04
4	4/3/2016	4/5/2016	Landsat-8	33.9	49.7	26.43	11822	3907	33.05	0.69	0.02	0.49	0.02	0.51	0.02
4	4/3/2016	4/5/2016	Landsat-8	33.9	49.7	26.43	16525	4643	28.10	0.75	0.04	0.55	0.03	0.56	0.03
2	4/4/2016	4/6/2016	Landsat-8	36.6	51.5	22.86	9992	2896	28.99	0.39	0.01	0.12	0.01	0.19	0.01
2	4/4/2016	4/6/2016	Landsat-8	36.6	51.5	22.86	7337	2255	30.74	0.43	0.05	0.16	0.05	0.23	0.05
1	4/20/2016	4/25/2016	Landsat-8	0.3	84.8	22.83	14180	4615	32.54	0.66	0.07	0.44	0.07	0.47	0.05
1	6/23/2016	6/25/2016	Landsat-8	0.0	66.2	14.76	6260	3575	57.11	0.58	0.06	0.33	0.07	0.38	0.06
1	6/23/2016	6/25/2016	Sentinel-2	0.0	66.2	14.76	6260	3575	57.11	0.49	0.07	0.26	0.04	0.31	0.05
4	7/11/2016	7/12/2016	Sentinel-2	0.0	97.1	26.13	5023	3443	68.53	0.25	0.03	0.15	0.02	0.18	0.02
4	7/11/2016	7/12/2016	Sentinel-2	0.0	97.1	26.13	6565	4690	71.43	0.25	0.02	0.15	0.01	0.18	0.01
1	7/25/2016	7/25/2016	Landsat-8	0.0	52.8	16.95	4780	3214	67.24	0.52	0.06	0.32	0.04	0.36	0.04
3	8/8/2016	8/8/2016	Sentinel-2	0.0	84.4	20.90	8146	5430	66.66	0.29	0.03	0.15	0.02	0.19	0.02
4	7/31/2016	8/9/2016	Sentinel-2	0.0	95.1	26.26	5411	4251	78.56	0.22	0.02	0.14	0.02	0.16	0.02
4	7/31/2016	8/9/2016	Sentinel-2	0.0	95.1	26.26	6141	4627	75.35	0.22	0.02	0.14	0.01	0.16	0.01
4	7/31/2016	8/9/2016	Sentinel-2	0.0	95.1	26.26	7724	6060	78.46	0.24	0.02	0.16	0.02	0.18	0.02

1	8/26/2016	8/26/2016	Landsat-8	0.0	62.4	19.01	5100	3140	61.57	0.44	0.03	0.29	0.02	0.32	0.02
1	8/26/2016	8/26/2016	Landsat-8	0.0	62.4	19.01	5111	3043	59.54	0.43	0.03	0.29	0.02	0.31	0.02
1	8/26/2016	8/26/2016	Landsat-8	0.0	62.4	19.01	5457	3309	60.65	0.46	0.04	0.29	0.06	0.32	0.04
1	8/17/2016	8/26/2016	Sentinel-2	11.0	71.0	18.76	5451	3109	57.04	0.47	0.06	0.27	0.03	0.32	0.03
1	8/17/2016	8/26/2016	Sentinel-2	11.0	71.0	18.76	5111	3043	59.54	0.37	0.06	0.21	0.04	0.25	0.04
1	8/17/2016	8/26/2016	Sentinel-2	11.0	71.0	18.76	5457	3309	60.65	0.42	0.05	0.24	0.03	0.29	0.03
1	9/11/2016	9/16/2016	Landsat-8	0.0	71.1	20.90	4800	3348	69.74	0.41	0.03	0.25	0.02	0.28	0.02
1	9/11/2016	9/16/2016	Sentinel-2	0.0	71.1	20.90	4800	3348	69.74	0.34	0.05	0.20	0.03	0.23	0.03
1	9/11/2016	9/19/2016	Landsat-8	0.0	71.1	20.90	3600	2794	77.60	0.41	0.03	0.25	0.02	0.28	0.02
1	9/11/2016	9/19/2016	Landsat-8	0.0	71.1	20.90	2800	2164	77.29	0.39	0.03	0.23	0.03	0.27	0.02
1	9/11/2016	9/19/2016	Landsat-8	0.0	71.1	20.90	2960	2298	77.63	0.44	0.04	0.27	0.03	0.30	0.03
1	9/11/2016	9/19/2016	Sentinel-2	0.0	71.1	20.90	3600	2794	77.60	0.31	0.04	0.17	0.02	0.21	0.02
1	9/11/2016	9/19/2016	Sentinel-2	0.0	71.1	20.90	2960	2298	77.63	0.32	0.05	0.19	0.03	0.22	0.03
1	9/11/2016	9/23/2016	Landsat-8	0.0	71.1	20.90	3520	1918	54.49	0.45	0.05	0.22	0.02	0.28	0.03
1	9/11/2016	9/23/2016	Landsat-8	0.0	71.1	20.90	5760	4282	74.35	0.43	0.05	0.23	0.04	0.28	0.04
1	9/11/2016	9/23/2016	Sentinel-2	0.0	71.1	20.90	3360	2532	75.36	0.30	0.06	0.15	0.04	0.19	0.04
1	9/11/2016	9/23/2016	Sentinel-2	0.0	71.1	20.90	5760	4282	74.35	0.33	0.06	0.17	0.04	0.21	0.04
1	9/11/2016	9/23/2016	Sentinel-2	0.0	71.1	20.90	3680	2530	68.76	0.39	0.06	0.20	0.03	0.25	0.04
1	9/21/2016	9/23/2016	Sentinel-2	6.3	57.7	21.46	3840	2466	64.23	0.29	0.04	0.18	0.03	0.21	0.03
1	9/21/2016	9/23/2016	Sentinel-2	6.3	57.7	21.46	4840	2919	60.31	0.33	0.05	0.20	0.03	0.23	0.03
1	9/21/2016	9/23/2016	Sentinel-2	6.3	57.7	21.46	4240	2765	65.20	0.31	0.04	0.18	0.03	0.21	0.03
1	9/21/2016	9/23/2016	Sentinel-2	6.3	57.7	21.46	3840	2612	68.02	0.31	0.05	0.18	0.03	0.22	0.03
4	9/29/2016	10/3/2016	Sentinel-2	141.2	53.2	25.96	14029	4237	30.20	0.45	0.04	0.29	0.03	0.32	0.03
4	9/29/2016	10/3/2016	Sentinel-2	141.2	53.2	25.96	9672	3017	31.19	0.51	0.04	0.33	0.03	0.36	0.03
1	10/21/2016	10/21/2016	Sentinel-2	0.0	78.1	24.03	5600	3760	67.14	0.36	0.06	0.17	0.03	0.22	0.04
1	10/21/2016	10/21/2016	Sentinel-2	0.0	78.1	24.03	5120	3680	71.87	0.37	0.06	0.19	0.03	0.24	0.04
1	10/21/2016	10/25/2016	Sentinel-2	0.0	78.1	24.03	7440	3190	42.88	0.30	0.05	0.15	0.03	0.19	0.03
1	10/21/2016	10/28/2016	Sentinel-2	0.0	78.1	24.03	2320	1134	48.87	0.34	0.06	0.16	0.03	0.21	0.04
1	10/21/2016	10/28/2016	Sentinel-2	0.0	78.1	24.03	4560	2575	56.47	0.30	0.05	0.13	0.02	0.17	0.03
1	10/21/2016	10/28/2016	Sentinel-2	0.0	78.1	24.03	6000	3132	52.20	0.35	0.07	0.16	0.04	0.21	0.04

1	10/21/2016	10/28/2016	Sentinel-2	0.0	78.1	24.03	9600	4732	49.30	0.39	0.05	0.18	0.03	0.24	0.03
1	11/20/2016	11/25/2016	Sentinel-2	126.2	41.5	22.12	5900	1716	29.09	0.65	0.08	0.40	0.11	0.44	0.08
1	11/20/2016	11/25/2016	Sentinel-2	126.2	41.5	22.12	7080	2647	37.39	0.38	0.13	0.28	0.08	0.29	0.09
1	11/20/2016	11/28/2016	Sentinel-2	126.2	41.5	22.12	4480	1129	25.21	0.61	0.05	0.4	0.05	0.43	0.04
1	11/20/2016	11/28/2016	Sentinel-2	126.2	41.5	22.12	5280	1518	28.76	0.52	0.09	0.11	0.07	0.19	0.08
1	11/20/2016	11/28/2016	Sentinel-2	126.2	41.5	22.12	10400	2315	22.26	0.71	0.05	0.46	0.07	0.50	0.05
1	11/20/2016	11/29/2016	Sentinel-2	126.2	41.5	22.12	9520	2707	28.44	0.48	0.08	0.32	0.06	0.35	0.06
4	3/21/2017	3/21/2017	Landsat-8	103.6	14.8	25.09	24789	4454	17.97	0.77	0.08	0.67	0.10	0.60	0.07
4	3/21/2017	3/21/2017	Landsat-8	103.6	14.8	25.09	27690	6068	21.91	0.80	0.04	0.70	0.07	0.62	0.04
4	3/21/2017	3/21/2017	Landsat-8	103.6	14.8	25.09	23151	5403	23.34	0.77	0.03	0.65	0.07	0.60	0.04
3	7/1/2017	7/3/2017	Landsat-8	0.0	91.8	17.8	8808	4417	50.15	0.64	0.05	0.38	0.02	0.44	0.02
3	6/24/2017	7/3/2017	Sentinel-2	0.0	91.5	18.49	8808	4417	50.15	0.60	0.04	0.36	0.03	0.41	0.03
3	9/19/2017	9/20/2017	Landsat-8	0.0	105.5	24.24	3222	2531	78.55	0.38	0.09	0.23	0.05	0.27	0.06
3	9/12/2017	9/20/2017	Sentinel-2	0.0	107.0	22.73	3222	2531	78.55	0.32	0.05	0.19	0.02	0.22	0.03
3	3/14/2018	3/22/2018	Landsat-8	77	69.1	24.53	10855	3120	28.74	0.79	0.03	0.57	0.05	0.58	0.03
3	3/16/2018	3/22/2018	Sentinel-2	108.2	59.3	24.14	10855	3120	28.74	0.69	0.04	0.47	0.05	0.49	0.04
3	4/25/2018	4/26/2018	Sentinel-2	0.4	63.5	20.38	13966	4576	32.77	0.60	0.05	0.38	0.04	0.42	0.04
2	12/15/2018	12/18/2018	Sentinel-2	0.0	60.0	26.71	14920	3090	20.71	0.69	0.05	0.49	0.04	0.50	0.03
2	12/15/2018	12/18/2018	Sentinel-2	0.0	60.0	26.71	20960	4043	19.29	0.80	0.05	0.62	0.05	0.60	0.04
2	12/15/2018	12/21/2018	Sentinel-2	0.0	60.0	26.71	20480	4232	20.66	0.71	0.05	0.51	0.04	0.52	0.04
2	1/4/2019	1/9/2019	Sentinel-2	146.4	38.3	26.05	34040	5206	15.29	0.84	0.03	0.69	0.03	0.64	0.02
2	1/4/2019	1/9/2019	Sentinel-2	146.4	38.3	26.05	42240	5285	12.51	0.85	0.02	0.70	0.03	0.65	0.02
3	1/10/2019	1/10/2019	Sentinel-2	44.3	35.8	23.81	12480	4480	35.90	0.72	0.04	0.52	0.04	0.53	0.03
2	1/19/2019	1/20/2019	Sentinel-2	0.0	81.8	28.71	14120	2841	20.12	0.56	0.04	0.42	0.04	0.42	0.04
3	1/28/2019	1/31/2019	Landsat-8	63.4	36.7	24.45	20840	5920	28.41	0.76	0.02	0.56	0.03	0.56	0.02
3	1/28/2019	1/31/2019	Landsat-8	63.4	36.7	24.45	17680	4600	26.02	0.77	0.01	0.59	0.02	0.58	0.01
3	1/28/2019	1/31/2019	Landsat-8	63.4	36.7	24.45	24080	6800	28.24	0.78	0.03	0.56	0.07	0.57	0.04
3	1/28/2019	1/31/2019	Landsat-8	63.4	36.7	24.45	26520	7600	28.66	0.79	0.02	0.59	0.07	0.58	0.04
2	2/8/2019	2/13/2019	Sentinel-2	122.6	63.0	27.65	34360	6590	19.18	0.72	0.07	0.53	0.07	0.53	0.06
2	2/8/2019	2/13/2019	Sentinel-2	122.6	63.0	27.65	37240	5492	14.75	0.79	0.05	0.60	0.05	0.59	0.04

3	2/9/2019	2/14/2019	Sentinel-2	26.4	37.0	24.35	19905	4180	21.00	0.68	0.06	0.48	0.05	0.50	0.05
2	2/8/2019	2/15/2019	Sentinel-2	122.6	63.0	27.65	25400	4252	16.74	0.78	0.03	0.56	0.03	0.57	0.02
2	2/8/2019	2/15/2019	Sentinel-2	122.6	63.0	27.65	24480	3413	13.94	0.78	0.03	0.57	0.04	0.57	0.03
2	2/23/2019	2/23/2019	Sentinel-2	49.8	42.0	26.68	32320	4581	14.17	0.88	0.04	0.67	0.06	0.65	0.04
2	2/23/2019	2/23/2019	Sentinel-2	49.8	42.0	26.68	26240	3581	13.65	0.89	0.03	0.67	0.06	0.65	0.03
2	2/23/2019	2/24/2019	Sentinel-2	49.8	42.0	26.68	33320	4999	15.00	0.88	0.03	0.66	0.06	0.65	0.04
2	2/23/2019	2/24/2019	Sentinel-2	49.8	42.0	26.68	32800	4421	13.48	0.89	0.01	0.62	0.06	0.63	0.03
3	2/24/2019	2/28/2019	Sentinel-2	152.5	17.9	22.64	25920	5080	19.6	0.85	0.04	0.68	0.05	0.64	0.03
3	3/6/2019	3/7/2019	Sentinel-2	171.3	14.1	21.72	36440	9080	24.92	0.78	0.03	0.56	0.03	0.57	0.02
3	3/6/2019	3/7/2019	Sentinel-2	171.3	14.1	21.72	33160	8520	25.69	0.78	0.04	0.56	0.05	0.57	0.04
3	3/6/2019	3/7/2019	Sentinel-2	171.3	14.1	21.72	34640	8920	25.75	0.81	0.02	0.61	0.03	0.60	0.02
3	3/6/2019	3/7/2019	Sentinel-2	171.3	14.1	21.72	24520	6720	27.41	0.81	0.01	0.61	0.02	0.60	0.01
3	4/2/2019	4/4/2019	Landsat-8	0.0	84.9	23.28	17760	4680	26.35	0.80	0.02	0.52	0.04	0.56	0.02
3	4/2/2019	4/4/2019	Landsat-8	0.0	84.9	23.28	16720	4840	28.95	0.78	0.03	0.52	0.04	0.55	0.03
3	4/2/2019	4/4/2019	Landsat-8	0.0	84.9	23.28	26600	5960	22.41	0.79	0.01	0.55	0.01	0.57	0.01

Validation dataset

4	11/11/2015	11/12/2015	Landsat-8	52.9	74.9	26.71	5859	2239	38.21	0.45	0.04	0.45	0.04	0.38	0.03
2	12/14/2015	12/22/2015	Landsat-8	181.4	40.6	22.24	14656	4946	33.74	0.68	0.03	0.42	0.06	0.47	0.04
2	12/14/2015	12/22/2015	Landsat-8	181.4	40.6	22.24	11618	4177	35.96	0.66	0.04	0.44	0.05	0.47	0.04
3	2/21/2016	3/1/2016	Landsat-8	55.9	33.5	23.77	20503	6086	29.68	0.8	0.04	0.6	0.11	0.59	0.04
2	4/4/2016	4/6/2016	Landsat-8	36.6	51.5	22.86	8574	2616	30.52	0.49	0.08	0.24	0.09	0.30	0.08
4	7/11/2016	7/12/2016	Sentinel-2	0.0	97.1	26.13	7805	5121	65.62	0.28	0.03	0.17	0.02	0.20	0.02
3	7/30/2016	8/8/2016	Landsat-8	0.0	91.7	20.46	8146	5430	66.66	0.42	0.10	0.22	0.05	0.28	0.06
1	8/26/2016	8/26/2016	Landsat-8	0.0	62.4	19.01	5451	3109	57.04	0.51	0.05	0.33	0.02	0.36	0.02
1	8/17/2016	8/26/2016	Sentinel-2	11.0	71.0	18.76	5100	3140	61.57	0.38	0.04	0.22	0.03	0.26	0.03
1	9/11/2016	9/19/2016	Sentinel-2	0.0	71.1	20.90	2800	2164	77.29	0.30	0.05	0.16	0.03	0.20	0.03
1	9/11/2016	9/23/2016	Landsat-8	0.0	71.1	20.90	3360	2532	75.36	0.40	0.04	0.21	0.02	0.26	0.03
1	9/11/2016	9/23/2016	Landsat-8	0.0	71.1	20.90	3680	2530	68.76	0.49	0.04	0.27	0.03	0.32	0.03
1	9/11/2016	9/23/2016	Sentinel-2	0.0	71.1	20.90	3520	1918	54.49	0.36	0.07	0.17	0.03	0.22	0.04

4	9/29/2016	10/3/2016	Sentinel-2	141.2	53.2	25.96	10842	3560	32.83	0.51	0.03	0.33	0.02	0.36	0.02
1	10/21/2016	10/21/2016	Sentinel-2	0.0	78.1	24.03	7120	4462	62.67	0.37	0.05	0.19	0.03	0.24	0.03
1	10/21/2016	10/25/2016	Sentinel-2	0.0	78.1	24.03	7820	3315	42.39	0.33	0.06	0.15	0.03	0.20	0.04
1	11/20/2016	11/28/2016	Sentinel-2	126.2	41.5	22.12	7520	2095	27.87	0.71	0.06	0.45	0.07	0.49	0.05
1	11/20/2016	11/29/2016	Sentinel-2	126.2	41.5	22.12	9920	2836	28.59	0.51	0.16	0.34	0.10	0.37	0.11
2	12/15/2018	12/21/2018	Sentinel-2	0.0	60.0	26.71	20200	4993	24.72	0.75	0.03	0.56	0.03	0.56	0.02
3	1/10/2019	1/10/2019	Sentinel-2	44.3	35.8	23.81	13920	4600	33.05	0.86	0.04	0.70	0.05	0.66	0.04
3	1/10/2019	1/13/2019	Sentinel-2	44.3	35.8	23.81	13290	4040	30.40	0.79	0.08	0.61	0.10	0.59	0.07
2	1/19/2019	1/20/2019	Sentinel-2	0.0	81.8	28.71	25840	6371	24.66	0.55	0.02	0.41	0.02	0.41	0.02
3	2/24/2019	2/28/2019	Sentinel-2	152.5	17.9	22.64	32400	7240	22.35	0.85	0.03	0.67	0.04	0.64	0.03
3	4/2/2019	4/4/2019	Landsat-8	0.0	84.9	23.28	29440	5520	18.75	0.79	0.01	0.55	0.02	0.57	0.01

AFB: Aboveground fresh biomass; ADB: Aboveground dry biomass; DMC: Dry matter concentration

CHAPTER 2 - A new approach for grazing management and stocking rate adjustment in Mombaça guinea grass pastures using satellite imagery and machine learning.

Article under review in Precision Agriculture (2022)

Graphical abstract

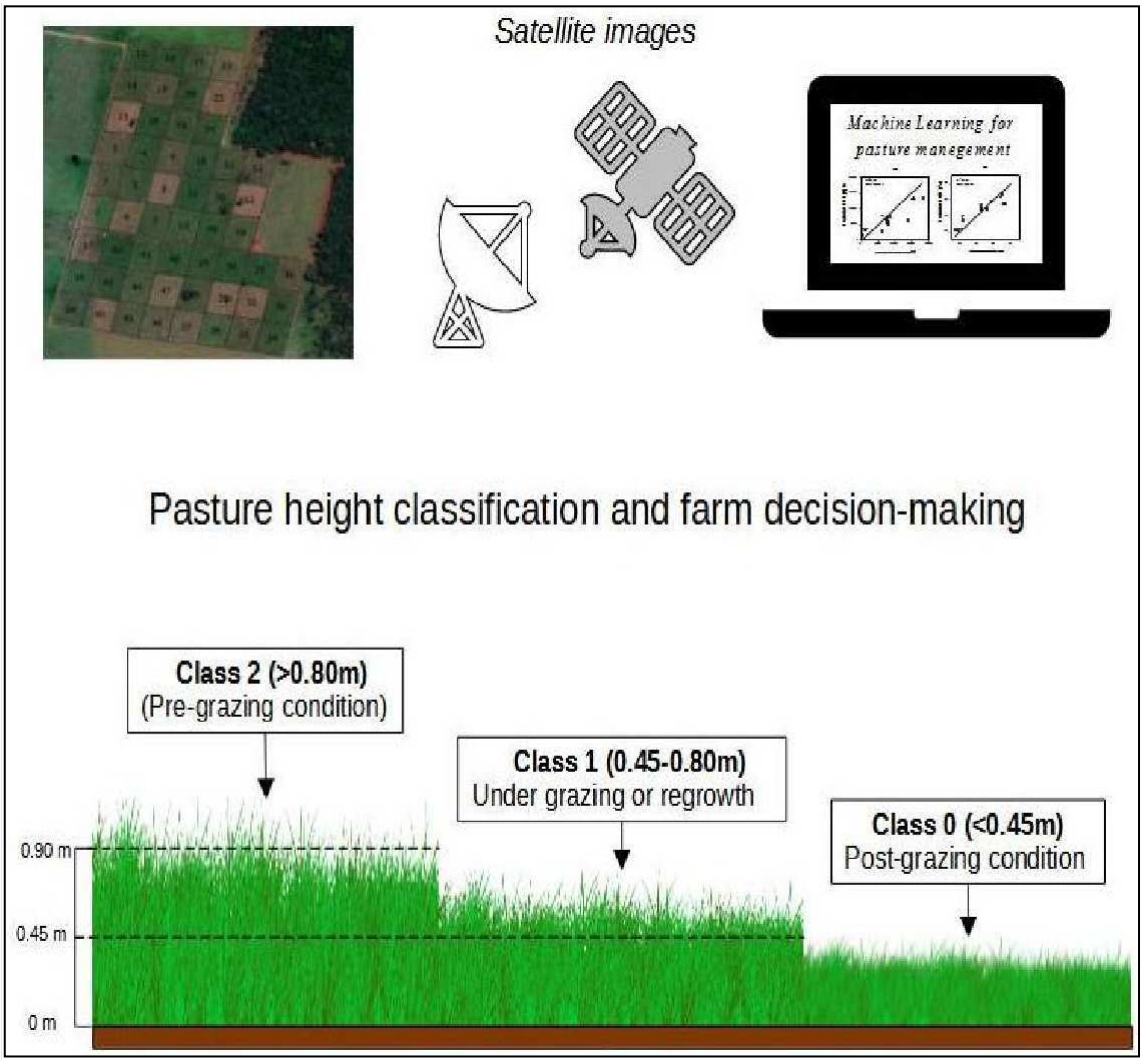

Abstract

Advances in pasture management can serve an important role in increasing production efficiency and sustainability. In this study, we aimed to develop a model for automated height classification and evaluate the accuracy of indirect estimates of forage biomass in Mombaça guinea grass (*Megathyrsus maximus* cv. Mombaça) pastures. This model is based on the analysis of images obtained through the Sentinel-2 satellite using machine learning techniques to support decision-making regarding grazing management and stocking rate adjustment. We

used different bands from the Sentinel-2 satellite that were obtained and processed entirely in the cloud. Three forage height classes were previously defined as class 0 (<45cm), class 1 (45–80cm) and class 2 (>80cm) according to management recommendations. The random forest algorithm was used to classify forage height and predict biomass by using height and biomass field data obtained from 54 paddocks in Brazil between 2016 and 2018 as reference data. The results demonstrate precision, recall, and accuracy values of up to 83, 90, and 83%, respectively, for paddock height classification and the potential to accurately predict aboveground fresh biomass (AFB) and dry matter concentration (DMC; R^2=0.69 and 0.82, respectively). We conclude that the combined use of satellite imagery and machine learning techniques makes it possible to classify height and predict the biomass of Mombaça guinea grass (*Megathyrsus maximus* cv. Mombaça) accurately while supporting decision-making regarding grazing management and stocking rate adjustment. However, further studies should be conducted to improve the proposed models and software should be developed to implement the tool under field conditions.

Keywords: Livestock precision farming. Forage height. Pasture biomass. Pasture management. Remote sensing. Tropical grasslands

Introduction

The growth prospects of the global population and consequent demand for food—especially products of animal origin—impose new challenges for the agricultural sector. It is estimated that food production will need to increase by up to 70% by 2050 to meet this demand (FAO, 2009). Additionally, there is growing global concern regarding issues related to the reduction of environmental impacts caused by livestock, which highlights the need to improve animal production efficiency.

Pastures occupy approximately one-third of the earth's surface, represent most of the arable land on the planet, and are mainly used for livestock (Reinermann et al. 2020). In Brazil, pastures occupy approximately 160 million hectares (IBGE 2017) and represent the basis of feed for most national herds. Thus, pastures are important contributors to animal product supply and ecosystem services (O'Mara 2012). Advances in pasture management can serve an important role in increasing targeted production efficiency and sustainability (Zhang et al. 2018; Nickmilder et al. 2021).

However, the current global scenario is one of increasing herds per farm or unit of pasture area (ABIEC 2020; Ellis et al. 2020). Associated with this, an increasing shortage of labor in the agricultural sector is expected (Bêrni et al. 2006). Such factors reduce the capacity for continuous monitoring and large-scale data collection, which are essential for optimizing management within animal production systems—especially in pastures, which often have large extensions, difficult access, and high spatial and temporal variability in terms of biomass, botanical composition, and relief (Bretas et al. 2021).

In this context, the advent of new technologies such as sensors onboard drones or satellites allows continuous data collection on a large scale, remotely, and at a low cost. Additionally, growing advances in cloud computing, the internet of things (IoT), artificial intelligence, machine learning, and data mining techniques generally allow individuals to obtain insights that support decision-making in the field in a fast and automated manner.

In terms of pasture management, there is a consensus in the literature that grazing management should be based on the average height of the pasture according to goals established based on the forage species intercepting 95% of incident light (IL_{95}). This recommendation is due to the correlations between height and leaf area index, mass, and the nutritional value of the forage, which characterizes the IL_{95} value. Notably, IL_{95} is used as a criterion for interrupting the period of pasture regrowth (Hodgson, 1990; Carnevalli et al. 2006; Da Silva et al. 2015; Da Silva et al. 2020). Similarly, adjustments to stocking rates to ensure high animal performance and perennial pastures should be based on the relationship between the nutritional requirements of animals and pasture biomass as a way to avoid overgrazing or under grazing conditions that compromise forage harvesting efficiency (Bretas et al. 2021). However, the traditional method used to obtain the average canopy height of a pasture is based on measurements of height in the field using a graduated ruler, while biomass is typically estimated through the destructive sampling of a pasture with the aid of frames of a known area, making these methods laborious, time-consuming, and costly due to low operational capacity (Catchpole and Wheeler 1992; Borra-Serrano et al. 2019).

Several recent works have demonstrated the potential for accurately predicting pasture biomass through remote sensing (Wang et al. 2017; Punalekar et al. 2018; Batistoti et al. 2019; Otgonbayar et al. 2019; DiMaggio et al. 2020; Bretas et al. 2021). However, there remain gaps in knowledge on tropical grasses, such as models for predicting the biomass of Mombaça guinea grass (*Megathyrsus maximus* cv. Mombaça). Furthermore, in the light of our current

knowledge, no work has been conducted to develop models for classifying forage height that allow for automated grazing management in intermittent stocking systems.

Species of the genus *Megathyrsus*—especially Mombaça guinea grass (*Megathyrsus maximus* cv. Mombaça)—are among the most commonly used in intensive systems in Brazil due to their high potential for the production of forage with high nutritional value (Fernandes et al. 2014; Pereira et al. 2021). However, species of this genus require the continuous monitoring of pasture structure to ensure greater grazing efficiency, which requires further studies linked to the greater automation of management.

The present study aimed to (I) develop a model for automated canopy height classification and (II) evaluate the accuracy of indirect estimates of forage biomass in Mombaça guinea grass (*Megathyrsus maximus* cv. Mombaça) based on the analysis of images obtained through the Sentinel-2 satellite using machine learning techniques to support decision-making regarding grazing management and stocking rate adjustment.

Materials and methods

Description of the experimental area

The study was conducted at Embrapa Gado de Corte, Campo Grande - MS (20º27'S, 54º37'W and altitude of 530 m) from March 2016 to November 2018. According to the Köppen classification, the climate of the study area is tropical savanna, subtype Aw, characterized by the seasonal distribution of rainfall. The average annual rainfall is approximately 1,500 mm, with 80% of the rain concentrated between the months of October to April. The historical average minimum and maximum temperatures (1993–2013) are 15.3 and 27.3°C in the coldest months and 18.2 and 31.2°C during the summer, respectively. Rainfall and minimum, average, and maximum temperatures throughout the study period were recorded by the Embrapa Gado de Corte meteorological station, located approximately 4 km from the experimental area (Figure 1). The soil of the study area is classified as red latosol, with a clay content ranging between 30 and 35%.

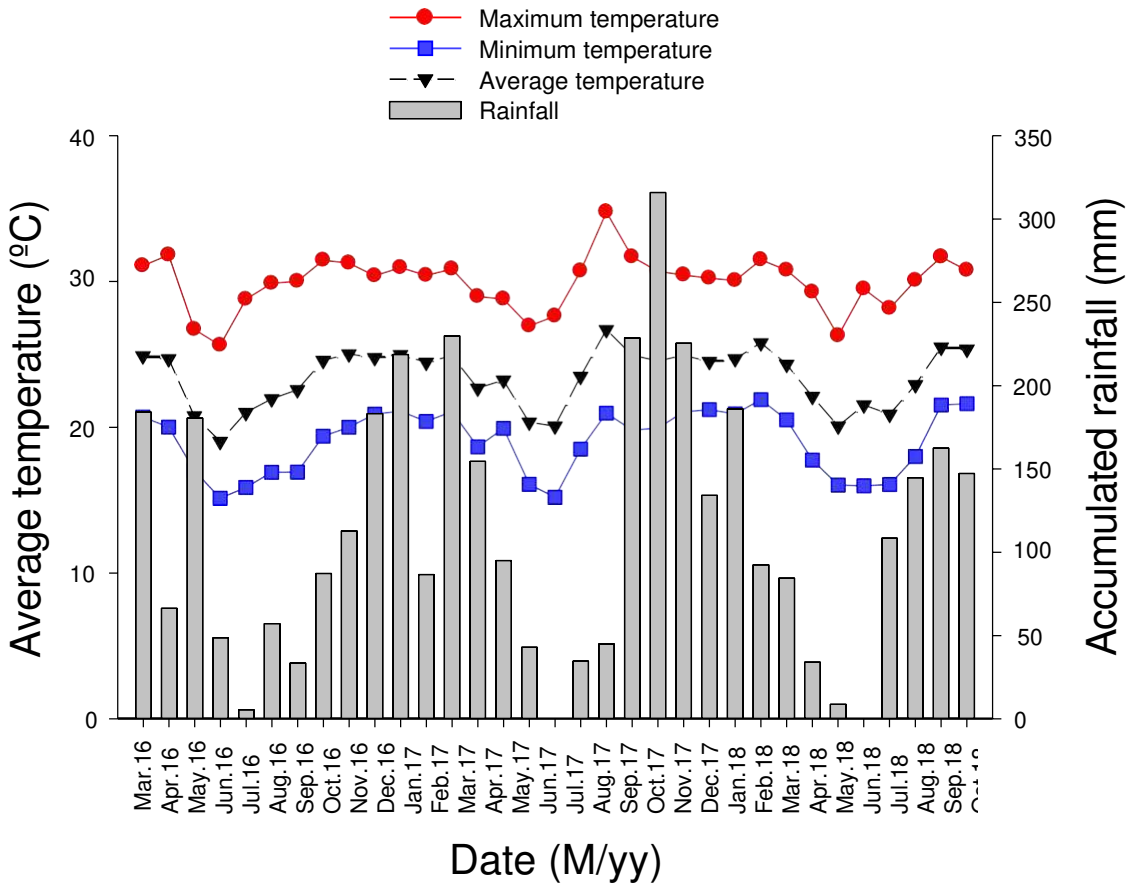

Fig. 1 Monthly accumulated precipitation and average temperature data over the experimental period

The experimental area is located in the Cerrado biome, occupies about 13.5 ha, and was divided into three blocks. Each block was subdivided into three modules of six paddocks, totaling 54 paddocks of 0.25 ha each (Figure 2). The area was established between 2008 and 2010 with the grass Mombaça guinea grass (*Megathyrsus maximus* cv. Mombaça) and used since then under intermittent stocking with beef cattle. The paddocks received three different annual doses of nitrogen in the form of urea (100, 200, and 300 kg ha^{-1}) during the evaluations, in addition to topdressing with 80 kg ha^{-1} of P_2O_5 and 80 kg ha^{-1} of K_2O. The different doses were used to ensure greater variability in the dataset used for modeling.

Throughout the study period, the area was managed under intermittent stocking with variable stocking rates. Fifty-four male of Nelore breed were used (mean initial live weight: 205 ± 26 kg), which remained in the paddocks throughout the experimental period and had access to water and mineral salt *ad libitum*. An extra paddock of approximately 6 ha, formed predominantly by *Megathyrsus maximus* cv. Massai was used as a reserved area for management adjustments in the "put and take" system. A canopy height of 80–90 cm was used as the criterion to start grazing in each of the paddocks. Stocking was adjusted to maintain a

post-grazing canopy height of 40–45 cm, following the recommendations of Euclides et al. (2015) and Alvarenga et al. (2020).

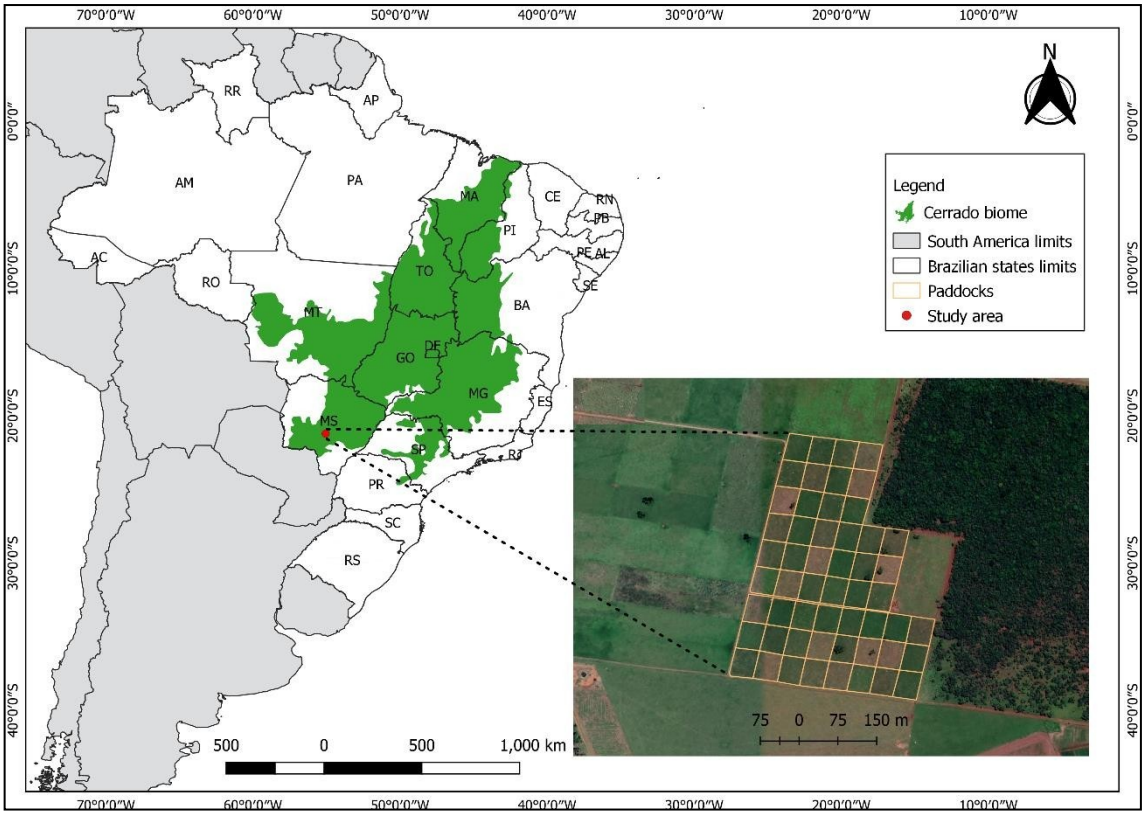

Fig. 2 Location map of the study area

Field data collection

Pasture evaluations were conducted in the paddocks of each module during each grazing cycle. Thus, height measurements and the quantification of pasture biomass were performed in nine paddocks (3 modules x 3 blocks) in pre- and post-grazing conditions for each cycle.

Forage height was determined using a ruler (graduated in centimeters) at 40 points that were randomly chosen in each paddock. The canopy height at each point corresponded to the average height of the curvature of the leaves around the ruler, while the height of the pasture was determined by the average between the 40 measured points.

The forage mass was estimated by cutting all the forage contained within nine frames (1 m²) randomly thrown into the respective paddocks. The samples were packed in paper bags, weighed, and dried in an oven with forced air ventilation at 55ºC until constant weight. They were then weighed again to determine the dry mass of forage.

Stocking adjustments were performed weekly depending on the relationship between the average weight of the animals and the forage height and biomass in the respective paddocks.

All the forage height and biomass field data were provided by Embrapa Gado de corte to modeling.

Acquisition and processing of satellite data

Data from the Sentinel-2 satellite were obtained and processed entirely in the cloud through the Google Earth Engine (GEE) platform. The Sentinel-2 satellite is operated by the European Space Agency (ESA) and provides free images in 13 spectral bands (490–2190 nm), with a temporal resolution of 5 days and a spatial resolution of 10m (bands 2, 3, 4, and 8) and 20m (bands 5, 6, 7, 8A, and 11) for the main bands used for agricultural monitoring. The spectral wavelengths available in Sentinel-2 and used in the present study are 490, 590, 665, 705, 740, 783, 842, 865, and 1610 nm, in ascending band order. Although the area had been under the same management since 2014, Sentinel-2 was only launched in June 2015, with data becoming available on the GEE platform from March 2016.

We used the Python programming language to automate vegetation reflectance data collection for each of the aforementioned bands. The vector layer of each of the paddocks was previously delimited using QGIS 3.16® software. Thus, for each of the paddocks on the respective dates, the value of each band was automatically obtained as the average between the pixels contained within the paddock limits.

After obtaining all available data between 03/2016 and 11/2018, we performed filtering based on cloud cover and the intervals between the dates of image acquisition and field data collection in the respective paddocks. As a criterion for filtering the satellite data, we used a maximum probability of 10% of the pixels covered by clouds and two levels of restriction for date ranges between image and field sampling (DR): 1 and 5 days (DR1 and DR5, respectively). In this way, two data sets were constructed (maximum date ranges of 1 and 5 days, respectively) and all images used were obtained before field sampling and considered cloud-free. Although filtering the data significantly reduced the database available for modeling, we understand that cloud-covered images can yield biased results. Regarding the restriction for the difference between dates, we considered the high growth rate of Mombaça guinea grass (*Megathyrsus maximus* cv. Mombaça) when under favorable conditions. Thus, we hypothesized that images obtained long in advance may not portray the current condition of the pasture.

Modeling

For the development of models for height classification and the prediction of pasture biomass, all of the aforementioned individual bands (9) and all possible combinations between bands of the Sentinel-2 satellite by difference, normalization, or division were calculated according to equations 1, 2, and 3, respectively, totaling 108 combinations (36×3).

$$DDoommooinnSSiioonnoo\ ooyy\ mmiiRRRReeTTeennccee = BB_{XX} - BB_{yy} \quad (1)$$

$$DDoommooinnSSiioonnoo\ ooyy\ nnooTTmmSSiizzSSiioonn = \frac{(BB_{XX} - BB_{yy})}{(BB_{XX} + BB_{yy})} \quad (2)$$

$$DDoommooinnSSiioonnoo\ ooyy\ mmivviiioonn = \frac{BB_{XX}}{BB_{yy}} \quad (3)$$

where BB_{XX} and BB_{yy} represents the two different bands combined.

Additionally, different vegetation indices described in the literature and commonly used for vegetation monitoring were calculated, resulting in 145 features from combinations between bands. The main indices from the literature calculated in the current study are represented in Supporting information 1 (S1). The date range and the other 145 aforementionedfeatures were used to correlate the height data obtained in the field at the corresponding dates and paddocks.

In addition to the 145 features obtained from reflectance data and the date range used for height classification models, season and paddock condition (pre- or post-grazing) were also used as predictor features for biomass models, totaling 148 predictive features in this case.

For modeling, the original database was randomly divided into training data (75%) and test data (25%). The training dataset was used to perform all modeling steps (data pre-processing, variable selection, and hyperparameter optimization). The number of predictor features in the model was defined for each of the datasets (DR1 and DR5) based on the balanced accuracy metric (classification) or root mean square error (RMSE; regression). To select the predictor features, we used K-folds (5-folds) cross-validation and the Recursive Feature Elimination – Cross-Validation (RFECV) tool. RFECV selects the best subset of features based on the model's cross-validation score to recursively eliminate minor features. After the selection of features, the hyperparameter optimization of the model was performed using the Bayesian optimization function of the Scikit-Optimize Library (version 0.7.4). After all of the modeling steps, the test dataset was applied to the final model for height classification and biomass prediction.

For both forage height classification and biomass regression, we used the random forest algorithm. This is because results from several studies (Mutanga et al. 2012; Wang et al. 2017; Bretas et al. 2021) demonstrated the better performance of the random forest algorithm when compared to other techniques for pasture research. The “Classifier” and “Regressor” functions of the algorithm were adopted according to the modeling objectives. All statistical analyses were conducted in Python 3 (version 3.7). A flow chart of data acquisition and modeling is presented in Figure 3.

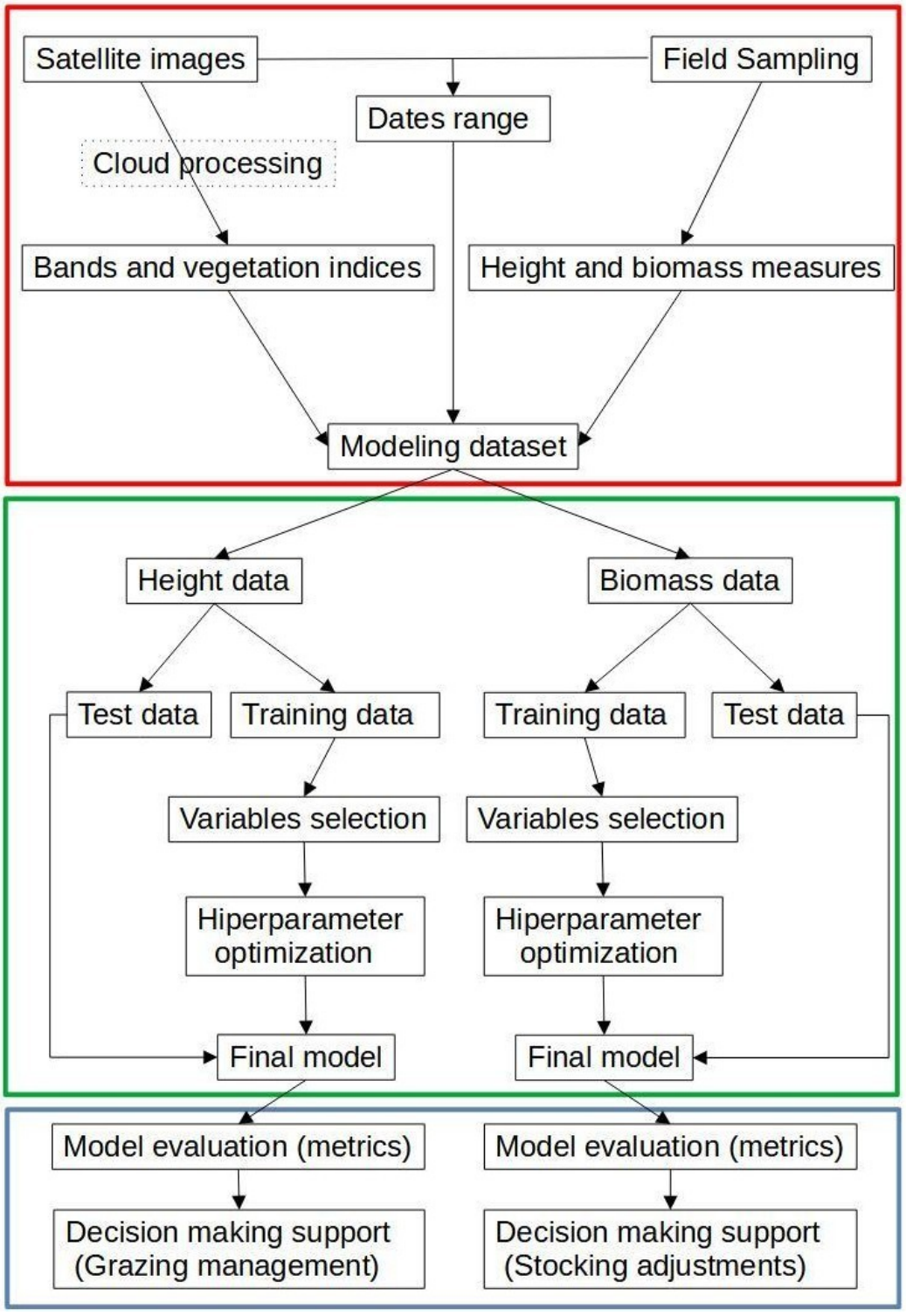

Fig. 3

Flow chart of data acquisition and modeling for forage height classification and biomass prediction. The red box represents the acquisition data step, the green box represents the modeling step, and the blue box represents the interpretation of results

Supervised classification of forage height

After filtering the satellite images, databases with 149 (DR5) and 51 height observations (DR1), respectively, were used to develop the automated classification model.

To develop the supervised sward height classification model, three classes were previously determined: Class 0 (<45cm), 1 (45–80cm), and 2 (>80cm). The height classes were defined based on the recommended management height ranges for the grass in question (Carnevalli et al. 2006; Euclides et al. 2015; Da Silva et al. 2020; Alvarenga et al. 2020). In summary, class 0 represents the moment to stop grazing and move the animals to another paddock, class 1 indicates maintenance of the current state (i.e.: regrowth or grazing), and class 2 represents the possibility of entry of the animals into the paddock to begin grazing.

Model evaluations were performed based on different metrics calculated from the confusion matrix of the test data. The metrics used to evaluate the models are presented in Table 1.

Table 1 Metrics calculated for the evaluation of the classification model

Metric	Equation
Accuracy	(TP + TN) / (TP + TN + FP + FN)
Precision	TP / (TP + FP)
Recall	TP / (TP + FN)
F1 – Score	2 * (Recall * Precision) / (Recall + Precision)
Kappa coeficiente	(Agree - Chance Agree) / (1 - Chance Agree)

TP = True positive; TN = True negative; FP = False positive; FN = False negative

We chose to calculate different metrics to avoid erroneous interpretations of the models. The global accuracy represents the percentage of correct predictions of the model. However, it can lead to erroneous evaluations when there are classes with a low number of observations. Precision and recall are important for characterizing the impact of false positives and false negatives, respectively. However, these measures are considered contradictory, and an increase in one of the metrics leads to a decrease in the other. Thus, it is important to represent the F1 – score as a metric that considers the harmonic mean between precision and recall. The Kappa coefficient can facilitate the evaluation of the confusion matrices of models that involve three or more classes, as in the case of the present study.

Biomass prediction

After filtering the satellite images, a database of 166 biomass observations (DR5) obtained from the field, as well as another database with 64 observations (DR1), were used to develop the prediction model using supervised regression.

The predictive performance of the models was evaluated by predicting the aboveground fresh biomass (AFB), aboveground dry biomass (ADB), and dry matter concentration (DMC) for the test dataset using the coefficient of determination (R^2) and the RMSE. Such metrics are widely used to evaluate prediction models of the biophysical features of vegetation and were calculated based on equations 4 and 5, as described by Richter et al. (2012).

$$RR^2 = 1 - \frac{\sum_{ii=1}^{mm} (VV_{000000}^{ii} - \hat{V}_{eeeee})^2}{\sum_{ii=1}^{mm} (VV_{000000}^{ii} - \bar{V}_{000000})^2} \quad (4)$$

where VV_{000000}^{ii} is the observed variable, $\hat{V}_{eeeee}$ is the model prediction, and $\bar{V}_{000000}$ is the average of the observed features.

$$RRMMMMEE = \sqrt{\frac{1}{nn} \sum_{ii=1}^{nn} (\hat{V} - VV^{ii})^2} \quad (5)$$

where nn is the number of observed features.

Results

Height classification

Selection of features

In general, all bands of the Sentinel-2 satellite used in the present study proved to be important for the automated classification of Mombaça guinea grass (*Megathyrsus maximus* cv. Mombaça) height since all bands appear among the features selected for the model in isolation, or combinations between them (Figure 4). The importance attributed to the infrared band and the different bands of the red edge spectrum are highlighted. Notably, however, traditional indices described in the literature and commonly used for monitoring vegetation (e.g., normalized difference vegetation index - NDVI, enhanced vegetation index - EVI, green normalized difference vegetation index - GNDVI, and normalized difference red edge - NDRE) are not among the most important features for the model. For both models generated based on

the dataset defined by the DR5 and DR1 filters, 50 predictor features were selected based on the stabilization of the cross-validation score [see Supporting information 2 (S2)].

Changing the interval filter between image and sampling dates for DR1 had no impact on the number of selected features, but changed the features and their degree of importance for the model. The 20 main features selected for both models are represented in Figure 4, ranked by their degree of importance.

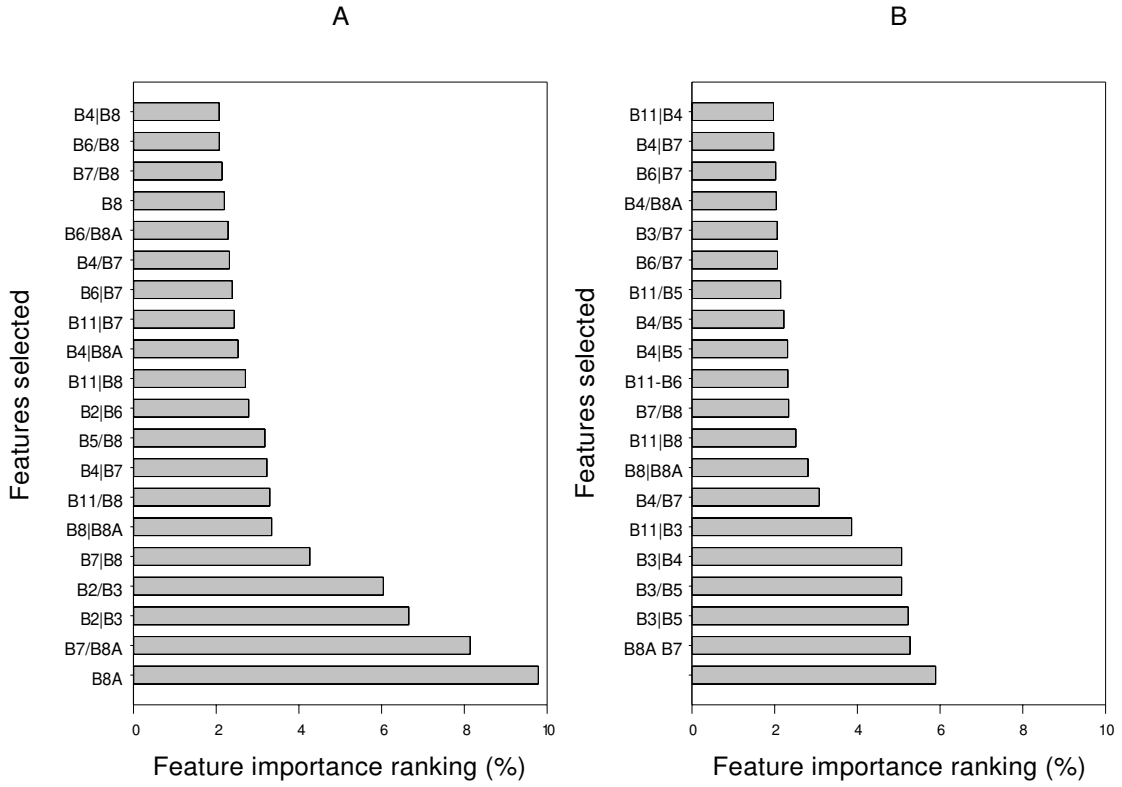

Figure 4 - Ranking of the most important features for height classification based on DR5 (a) and DR1 (b) datasets. B2 to B11 represent the different spectral bands obtained. The (-) signal represents the simple difference between bands, (/) represents the simple division between bands, and (|) represents the normalized difference between bands.

Model evaluation

The performance of the pasture canopy height classification model using the DR5 dataset can be assessed by the confusion matrix for the test data (Table 2).

Table 2 Confusion matrix based on test data for evaluating the classification model using the DR5 filter

		Predicted			Total
		Class 0	Class 1	Class 2	
Observed	Class 0	7	6	0	**13**
	Class 1	1	13	1	**15**
	Class 2	0	3	7	**10**
Total		**8**	**22**	**8**	**38**

Increasing the restriction for the interval between image acquisition and field sampling (DR1) showed important improvements in all metrics for the evaluation of the height classification model (Table 3).

Table 3 Confusion matrix based on test data for evaluating the classification model using the DR1 filter

		Predicted			Total
		Class 0	Class 1	Class 2	
Observed	Class 0	4	0	0	**4**
	Class 1	0	4	3	**7**
	Class 2	0	0	2	**2**
Total		**4**	**4**	**5**	**13**

Upon analyzing the confusion matrix for the smallest difference between dates (DR1), it was noted that every classification error occurred between classes 1 and 2, with the algorithm classifying paddocks that were still in class 1 (45–80cm) as being in class 2 (>80cm). Additionally, regardless of the interval between the dates used, there were no cases of confusion between classes 0 and 2 by the model. The metrics calculated based on the confusion matrices for the different date ranges between the imaging and sampling dates (DR5 and DR1) are represented in Table 4.

Table 4 Metrics calculated for cross-validation and test data based on the confusion matrices for the different intervals between the imaging and sampling dates (DR5 and DR1)

Item	DR5		DR1	
	Cross-validation (Training data)	Test data	Cross-validation (Training data)	Test data
Precision	0.66	0.69	0.60	0.83
Recall	0.64	0.69	0.61	0.90
Accuracy	0.49	0.67	0.68	0.83
F1 - score	0.68	0.71	0.63	0.83
Kappa coefficient	0.34	0.53	0.42	0.70

Biomass prediction

Selection of features

As observed for the development of the height classification model, most of the bands provided by the Sentinel-2 satellite were selected to predict the AFB and/or DMC of the forage (Figures 5 and 6). Additionally, the interval between image capture and field sampling dates, pasture condition (pre- or post-grazing), and season are among the features selected by the model. The features selected for the biomass prediction models are presented in Figures 5 and 6 (ranked by their degree of importance).

When using the DR5 dataset, 15 features were selected as predictors of AFB and 40 features were selected as predictors of DMC based on cross-validation scores. For the DR1 dataset, 20 features were selected as predictors of both AFB and DMC (see Supporting information 3 (S3)).

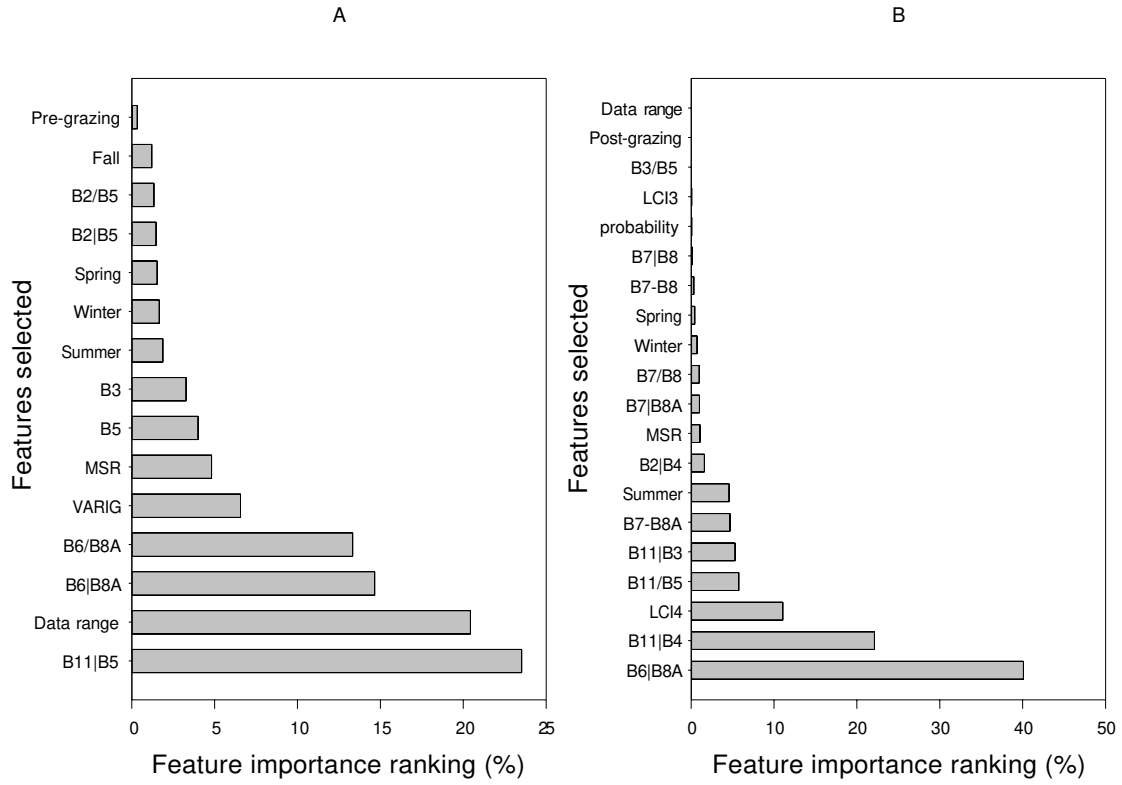

Fig. 5 Features selected by the AFB prediction model ranked by importance and based on the DR5 (a) and DR1 (b) datasets. B2 to B11 represent the different spectral bands obtained. The (-) signal represents the simple difference between bands, (/) represents the simple division between bands, and (|) represents the normalized difference between bands

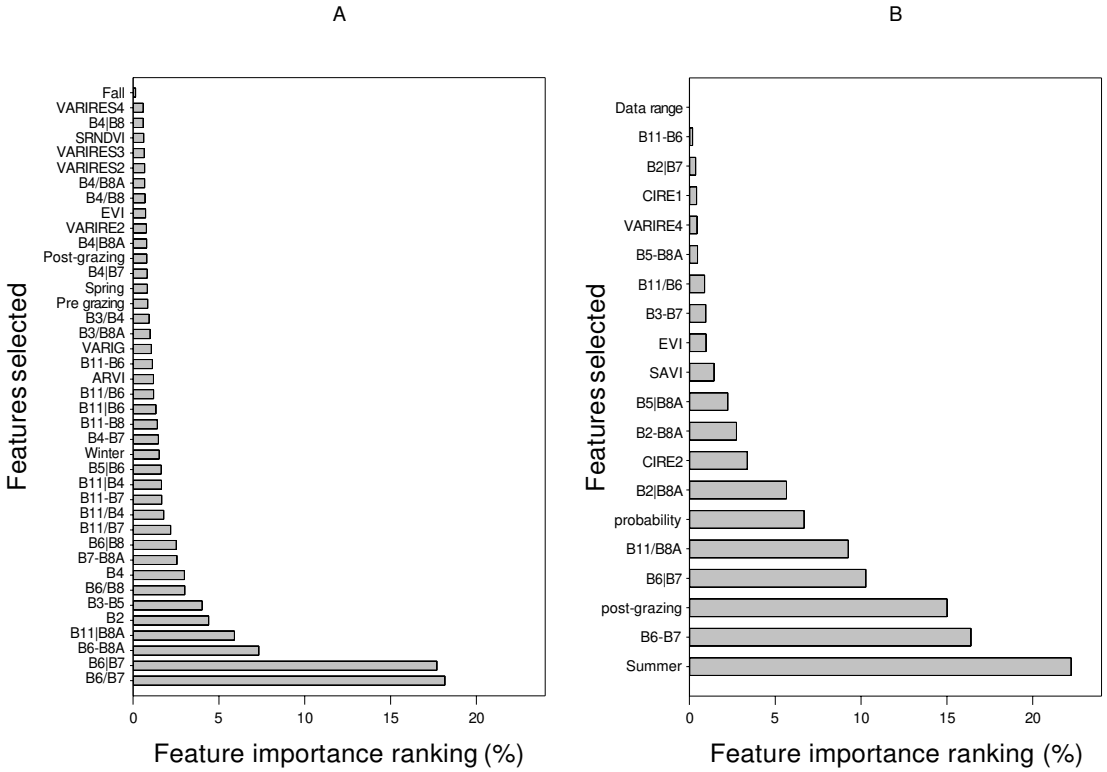

Fig. 6 Features selected by the DMC prediction model ranked by importance based on the DR5 (a) and DR1 (b) datasets. The (-) signal represents the simple difference between bands, (/) represents the simple division between bands, and (|) represents the normalized difference between bands

Model evaluation

Although the random forest algorithm did not show good performance for predicting the AFB (Figure 7a; R^2=0.27), it showed reasonable results for predicting the DMC (Figure 7b; R^2=0.62) when we used the DR5 dataset to develop the model.

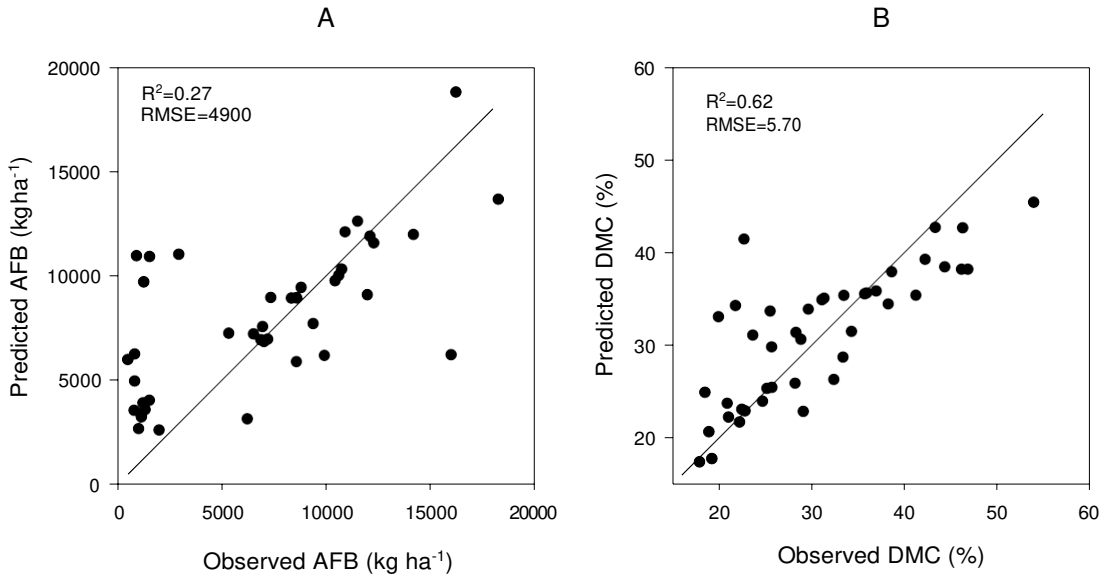

Fig. 7 Predictions of AFB (a) and DMC (b) based on test data using the random forest algorithm and maximum interval between image acquisition and field observation of 5 days (DR5).

When we increased the restriction for the difference between image acquisition and sampling dates (DR1), significant improvements in the performance of the prediction models for AFB (Figure 8A) and DMC (Figure 8B) were observed, as seen for the model classification of forage height.

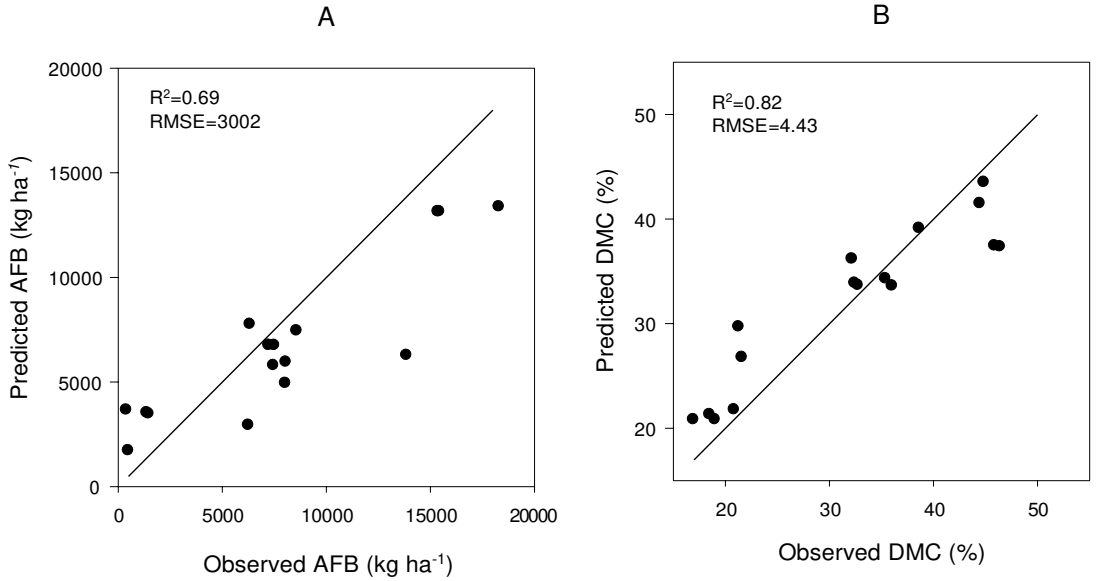

Fig. 8 Prediction of AFB (a) and DMC (b) based on test data using the random forest algorithm and maximum interval between image acquisition and field observation of 1 day (DR1).

Regardless of the dataset used for modeling (DR5 or DR1), we did not obtain satisfactory performance for aboveground dry biomass prediction (ADB; Figure 9).

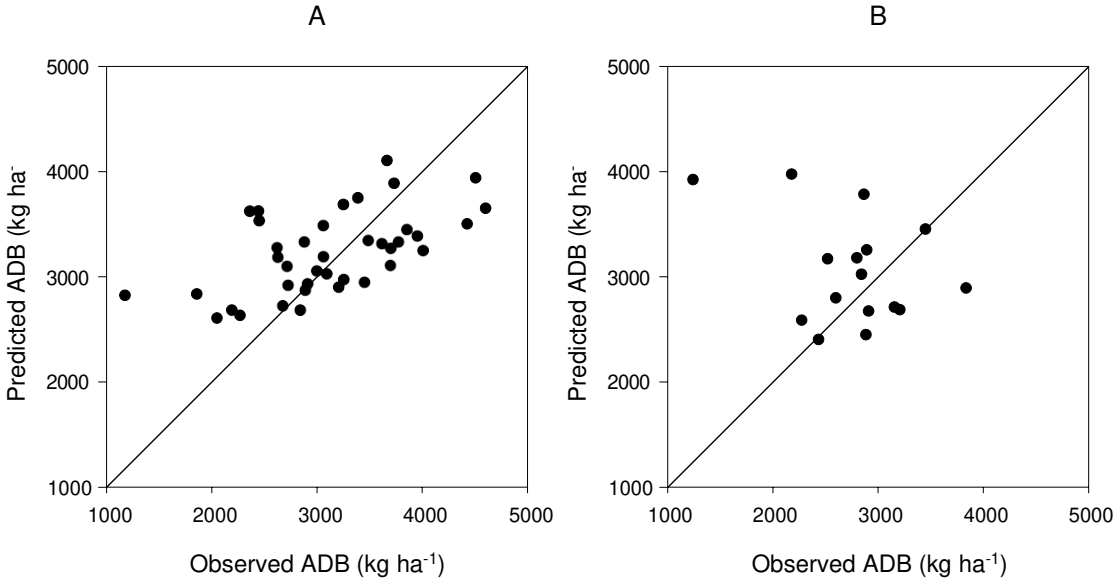

Fig. 9 Prediction of ADB based on data test using the random forest algorithm and maximum intervals between image acquisition and field observation of 5 (a) and 1 (b) days.

Discussion

Height classification

The features selected for the classification model of forage height of Mombaça guinea grass (*Megathyrsus maximus* cv. Mombaça) shows the greater relevance of reflectance data in the red edge and near-infrared range over data obtained in the visible range, thereby indicating the need to use multispectral sensors such as the Multispectral Instrument (MSI) sensor onboard the Sentinel-2 satellite. Imran et al. (2020) demonstrated the potential of the red edge band provided by the Sentinel-2 satellite for monitoring the structural heterogeneity of pastures, which corroborates the result of our study. Furthermore, Guerini Filho et al. (2020) used data from the Sentinel-2 satellite to estimate the biomass of tropical pastures and concluded that the red edge and near-infrared regions are crucial for improving the models. Due to the high correlation between biomass and height, it was expected that such regions of the electromagnetic spectrum would also stand out for the classification of forage height. On the other hand, Cimbelli and Vitale (2017) found a weak yet significant correlation between grassland height and the green, red, and near infrared bands obtained from the Sentinel-2 satellite. However, unlike in the present study, these authors did not evaluate the correlation between the bands in the red edge range or combinations between different bands. Additionally,

the ranking of the main features selected by the model suggests that new vegetation indices based on different combinations between bands may be more suitable for classifying forage height than some of the indices traditionally used for vegetation monitoring. Therefore, these new vegetation indices should be more thoroughly evaluated in new studies.

Regardless of the metric used for evaluation, the improved performance of the classification model when we reduced the interval between the dates of image acquisition and field sampling can be explained by the high growth rate of Mombaça guinea grass (*Megathyrsus maximus* cv. Mombaça), especially during the rainy season (Carnevalli et al. 2006; Fernandes et al. 2014; Pereira et al. 2021). Thus, paddocks classified based on a retroactive image may have undergone significant height changes during the days between image acquisition and field sampling. This result was expected and confirms the need for satellites with a high temporal resolution for this type of monitoring. Several studies have highlighted that adverse climatic conditions (e.g., cloud cover) and the resulting low temporal resolution are the main limitations of using satellites for pasture monitoring (Barret et al. 2014; Wang et al. 2019; Murphy et al. 2021). In these cases, an emerging alternative is the combined use of data from the Sentinel-2 satellite with the use of synthetic aperture radar (SAR) sensors onboard the Sentinel-1 satellite, which are capable of overcoming the limitations of lighting or cloud cover to ensure higher imaging frequency (Barret et al. 2014; Ali et al. 2017; Wang et al. 2019).

The confusion matrix for the test data based on the DR5 dataset demonstrates that most classification errors occurred between 0 and 1 or 1 and 2, thereby confirming our assumption that paddocks may have changed their condition over a period of 5 days. If we used an interval between dates greater than 5 days, errors between more discrepant classes (e.g., 0 and 2) could occur.

The evaluation metrics of the model developed based on images with a maximum interval of 1 day demonstrate good classification performance and a considerable balance between recall, precision, and accuracy. The data demonstrate that the development of new sensors capable of daily revisiting, or the acquisition of private plans for daily inspection, can guarantee the automation of grazing management with high accuracy. Additionally, classification errors occurred exclusively between classes 1 and 2, where paddocks with an actual height of 45–80cm were classified as paddocks above 80cm. In a simulation of decision-making regarding the management of grazing in the field, we understand that class 0 characterizes the moment of grazing interruption and driving the animals to another paddock. Class 1 implies maintenance of the current status of the paddock. That is, paddocks undergoing

regrowth must continue without animals until reaching class 2, while paddocks that are under grazing must continue with animals until reaching class 0. Class 2 represents the moment when grazing begins or the possibility of animals entering the paddock. Based on this simulation, the classification errors of the proposed model can be considered of lower impact since the animals would be moved to another paddock in an anticipated manner. This would imply a lower supply of forage and a shorter paddock occupation period. On the other hand, forage with better nutritional value and a greater number of grazing cycles is expected in the area since the anticipated movement of animals implies a greater residual area of leaves and a shorter interval required for regrowth. We believe that the delay in deciding whether or not to change the animals in the paddock would have more negative impacts since it would leave some paddocks in a condition of overgrazing and others with an unfavorable structure for animal consumption and low nutritional value. In summary, between classes 1 and 2, false positives for class 2 are have a lower impact on pasture management than false negatives for class 2.

We had great difficulties in finding scientific research involving the automated height classification of forage species with a focus on automated grazing management. However, we believe that the present work represents the initial development stage of an important tool for the management of pastures in intermittent stocking systems. Tiscornia et al. (2019) evaluated the correlation between reflectance data obtained by satellites and forage height measured in the field to estimate forage height via remote sensing and found a weak correlation. The same authors justified a low correlation due to the great variability in height within the same paddock and concluded that it is necessary to find new methods for monitoring height in pastures. In a review of technologies for optimizing pasture monitoring, Murphy et al. (2021) concluded that the main limitation of the remote sensing of pastures is their high heterogeneity (typically greater than in crops) where precision agriculture has been consolidated. On the other hand, Batistoti et al. (2019) and Obanawa et al. (2020) demonstrated high accuracy in predicting the height of pastures formed by grasses from tropical and temperate climates, respectively. However, these studies were conducted using a light detection and ranging (LiDAR) sensor in conjunction with unmanned aerial vehicles (UAV). While these are other potential technologies, their costs are relatively high and their use is restricted to small areas and with low wind interference (Vasquez-Arellano et al. 2016; Cooper et al. 2017; Murphy et al. 2021). In preliminary unpublished tests, we also did not obtain good predictive performance using regression models to predict forage height. Notably, we believe that classification based on the average height range of a paddock is sufficient for decision-making in grazing management.

Biomass prediction

The low performance of the AFB prediction model using the DR5 dataset was expected and can be explained by the long interval between the image acquisition date and the field observation, as discussed for the height classification model. Mombaça guinea grass (*Megathyrsus maximus* cv. Mombaça) is described as a forage with a high growth rate, especially during the rainy season, under favorable temperature and humidity conditions for growth (Carnevalli et al. 2006). Thus, images obtained more than 2 days in advance may not characterize the real condition of the pasture on the date of interest. Often, the period of occupation of a paddock established with this grass in Brazil is limited to an interval of 2 to 5 days. In the present study, the average daily growth rate of pasture during the summer was approximately 47 kg DM ha^{-1} day^{-1}, with a peak of up to 224 kg DM ha^{-1} day^{-1}. Figure 7A demonstrates the low accuracy of prediction for AFB below 5000 kg ha^{-1}. This is likely because the corresponding image characterized a condition of high biomass, yet the value observed in the field characterized a significant reduction of biomass after grazing for some days. Additionally, Figure 5 demonstrates the importance of the date range for predicting the AFB. On the other hand, the variation in forage DMC within a maximum interval of 5 days is less significant, which justifies the better performance of the model for DMC prediction. The importance attributed by the random forest algorithm to the season (especially summer) in the present study supports this justification.

Furthermore, improvement in the predictive performance of the models when we restricted the maximum interval between image acquisition and field observation to 1 day confirms the impact of changing pasture conditions in the short term when using images for modeling forage biomass—especially during the growing season.

The low performance of the model for predicting ADB observed in the present study was also previously described by Bretas et al. (2021), who justified the low predictive ability by the low variability in the dry biomass dataset used for modeling. The same authors explained that this low variability is due to the seasonal variation of forage structure and moisture. Therefore, during the annual dry period, a significant increase in the DMC of the plant compensates for the reduction in growth and biomass. During the growing season, the high biomass is contrasted with the low DMC of the plant, thereby making dry biomass values more homogeneous throughout the year. This explanation seems plausible since the coefficient of variation for the observed dry biomass dataset was approximately 25%, while the coefficient of

variation for the green biomass data was approximately 64%. Similar results were also found by Mundava et al. (2014), Pezzopane et al. (2019), and Tong et al. (2019).

While we understand that stocking adjustments in a pasture area must be made as a function of forage dry biomass, this does not make our model inefficient since accurate predictions of green biomass and forage dry matter percentage allow us to indirectly obtain dry biomass.

As an example of the practical application of the proposed model, we consider one of the paddocks (ID-48) of the study area shown in Figure 2. Results obtained by direct field sampling indicated an AFB of 10632 kg ha^{-1}, 28.92% DM, and forage biomass equal to 3075 kg DM ha^{-1}. For the same paddock, the values of AFB and DMC predicted by the proposed model were 9984.77 kg and 30.58%, respectively. This would result in an estimate of approximately 3053 kg DM ha, which is approximately 22 kg DM below the observed value. Such an estimate would allow us to adjust the paddock stocking according to animal demand in a fully automated and accurate manner. Several other authors have demonstrated the potential for the prediction of pasture biomass based on Sentinel-2 satellite images (Frampton et al. 2013; Punalekar et al. 2018; Guerini Filho et al. 2020; Bretas et al. 2021). However, none of these studies evaluated the accuracy of prediction for biomass among species of the genus *Megathyrsus*, which is frequently used in intensive grazing systems in Brazil.

Conclusions

The combined use of satellite images and machine learning techniques makes it possible to classify height and predict the biomass of Mombaça guinea grass (*Megathyrsus maximus* cv. Mombaça) accurately. However, this requires a high frequency of revisits by the satellite (daily) to achieve greater precision in decision-making related to pasture management.

Application of the forage height classification model, with the prediction of biomass based on free images processed completely in the cloud, would allow the unprecedented automation of pasture management. Thus, further studies should be directed toward improving the performance of these models and developing software or apps for implementing these tools in the field.

References

Ali, I., Barrett, B., Cawkwell, F., Green, S., Dwyer, E., & Neumann, M. (2017). Application of

Repeat-Pass TerraSAR-X Staring Spotlight Interferometric Coherence to Monitor Pasture Biophysical Parameters: Limitations and Sensitivity Analysis. *IEEE Journal of Selected Topics in Applied Earth Observations and Remote Sensing*, *10*(7), 3225–3231. https://doi.org/10.1109/JSTARS.2017.2679761

Alvarenga, C. A. F., Euclides, V. P. B., Montagner, D. B., Sbrissia, A. F., Barbosa, R. A., & De Araújo, A. R. (2020). Animal performance and sward characteristics of Mombaça guineagrass pastures subjected to two grazing frequencies. *Tropical Grasslands-Forrajes Tropicales*, *8*(1), 1–10. https://doi.org/10.17138/tgft(8)1-10

Associação Brasileira das indústrias exportadoras de carne – ABIEC (Brazilian Beef Exporters Association). 2020. Available online at: http://abiec.com.br/en/publicacoes/beef-report-2020-2/

Barrett, B., Nitze, I., Green, S., & Cawkwell, F. (2014). Assessment of multi-temporal, multi-sensor radar and ancillary spatial data for grasslands monitoring in Ireland using machine learning approaches. *Remote Sensing of Environment*, *152*, 109–124. https://doi.org/10.1016/j.rse.2014.05.018

Batistoti, J., Marcato Junior, J., Ítavo, L., Matsubara, E., Gomes, E., Oliveira, B., Souza, M., Siqueira, H., Salgado Filho, G., Akiyama, T., Gonçalves, W., Liesenberg, V., Li, J., & Dias, A. (2019). Estimating Pasture Biomass and Canopy Height in Brazilian Savanna Using UAV Photogrammetry. *Remote Sensing*, *11*(20), 2447. https://doi.org/10.3390/rs11202447

Berni, D. A.; Marquetti, A.; Peixoto, F. C. *Evolução setorial da economia brasileira entre 2002 e 2020: do passado ao futuro com o método Delphi (Sectorial evolution of the Brazilian economy between 2002 and 2020: from the past to the future with the Delphi method)*. Análise Econômica (UFRGS), v. 24, p. 183-210, 2006.

Borra-Serrano, I., De Swaef, T., Muylle, H., Nuyttens, D., Vangeyte, J., Mertens, K., Saeys, W., Somers, B., Roldán-Ruiz, I., & Lootens, P. (2019). Canopy height measurements

and non-destructive biomass estimation of *Lolium perenne* swards using UAV imagery. *Grass and Forage Science*, gfs.12439. https://doi.org/10.1111/gfs.12439

Bretas, I. L., Valente, D. S. M., Silva, F. F., Chizzotti, M. L., Paulino, M. F., D'Áurea, A. P., Paciullo, D. S. C., Pedreira, B. C., & Chizzotti, F. H. M. (2021). Prediction of aboveground biomass and dry-matter content in *Brachiaria* pastures by combining meteorological data and satellite imagery. *Grass and Forage Science*, *76*(3), 340–352. https://doi.org/10.1111/gfs.12517

Carnevalli, R. A., Silva, S. C. D., Bueno, A. A. O., Uebele, M. C., Bueno, F. O., Hodgson, J., Silva, G. N., & Morais, J. P. G. (n.d.). *Herbage production and grazing losses in Panicum maximum cv. Mombaça under four grazing managements*. 12.

Catchpole, W. R., & Wheeler, C. J. (1992). Estimating plant biomass: A review of techniques. *Austral Ecology*, *17*(2), 121–131. https://doi.org/10.1111/j.1442-9993.1992.tb00790.x

Cimbelli, A., & Vitale, V. (2017). Grassland Height Assessment by Satellite Images. *Advances in Remote Sensing*, *06*(01), 40–53. https://doi.org/10.4236/ars.2017.61003

Cooper, S., Roy, D., Schaaf, C., & Paynter, I. (2017). Examination of the Potential of Terrestrial Laser Scanning and Structure-from-Motion Photogrammetry for Rapid Nondestructive Field Measurement of Grass Biomass. *Remote Sensing*, *9*(6), 531. https://doi.org/10.3390/rs9060531

Da Silva, S. C., Bueno, A. A. O., Carnevalli, R. A., Silva, G. P., & Chiavegato, M. B. (2019). Nutritive value and morphological characteristics of Mombaça grass managed with different rotational grazing strategies. *The Journal of Agricultural Science*, *157*(7–8), 592–598. https://doi.org/10.1017/S0021859620000052

da Silva, S., Sbrissia, A., & Pereira, L. (2015). Ecophysiology of C4 Forage Grasses—Understanding Plant Growth for Optimising Their Use and Management. *Agriculture*, *5*(3), 598–625. https://doi.org/10.3390/agriculture5030598

DiMaggio, A. M., Perotto-Baldivieso, H. L., Ortega-S., J. A., Walther, C., Labrador-Rodriguez, K. N., Page, M. T., Martinez, J. de la L., Rideout-Hanzak, S., Hedquist, B. C., & Wester, D. B. (2020). A Pilot Study to Estimate Forage Mass from Unmanned Aerial Vehicles in a Semi-Arid Rangeland. *Remote Sensing*, *12*(15), 2431. https://doi.org/10.3390/rs12152431

Ellis, J., DeLong, K. L., Lambert, D. M., Schexnayder, S., Krawczel, P., & Oliver, S. (2020). Analysis of closed versus operating dairies in the southeastern United States. *Journal of Dairy Science*, *103*(6), 5148–5161. https://doi.org/10.3168/jds.2019-17516

Euclides, V. P. B., Lopes, F. da C., do Nascimento Junior, D., Carneiro da Silva, S., Difante, G. dos S., & Barbosa, R. A. (2016). Steer performance on Panicum maximum (cv. Mombaça) pastures under two grazing intensities. *Animal Production Science*, *56*(11), 1849. https://doi.org/10.1071/AN14721

FAO (2009). *How to Feed the World in 2050. High-Level Experts Forum*. Rome: FAO. Available online at: https://www.jstor.org/stable/25593700

Fernandes, F. D., Ramos, A. K. B., Jank, L., Carvalho, M. A., Martha Jr., G. B., & Braga, G. J. (2014). Forage yield and nutritive value of Panicum maximum genotypes in the Brazilian savannah. *Scientia Agricola*, *71*(1), 23–29. https://doi.org/10.1590/S0103-90162014000100003

Frampton, W. J., Dash, J., Watmough, G., & Milton, E. J. (2013). Evaluating the capabilities of Sentinel-2 for quantitative estimation of biophysical features in vegetation. *ISPRS Journal of Photogrammetry and Remote Sensing*, *82*, 83–92. https://doi.org/10.1016/j.isprsjprs.2013.04.007

Guerini Filho, M., Kuplich, T. M., & Quadros, F. L. F. D. (2020). Estimating natural grassland biomass by vegetation indices using Sentinel 2 remote sensing data. *International Journal of Remote Sensing*, *41*(8), 2861–2876.

https://doi.org/10.1080/01431161.2019.1697004

Hodgson, J. (1990). Grazing Management: Science into Practice. *Longman Scientific and Technical.*

Instituto Brasileiro de Geografia e Estatística (IBGE). (2017). *Censo Agropecuário (Agricultural Census)*. Available online at: https://biblioteca.ibge.gov.br/

Imran, H. A., Gianelle, D., Rocchini, D., Dalponte, M., Martín, M. P., Sakowska, K., Wohlfahrt, G., & Vescovo, L. (2020). VIS-NIR, Red-Edge and NIR-Shoulder Based Normalized Vegetation Indices Response to Co-Varying Leaf and Canopy Structural Traits in Heterogeneous Grasslands. *Remote Sensing*, *12*(14), 2254. https://doi.org/10.3390/rs12142254

Mundava, C., Helmholz, P., Schut, A. G. T., Corner, R., McAtee, B., & Lamb, D. W. (2014). Evaluation of vegetation indices for rangeland biomass estimation in the Kimberley area of Western Australia. *ISPRS Annals of the Photogrammetry, Remote Sensing and Spatial Information Sciences*, *II–7*, 47–53. https://doi.org/10.5194/isprsannals-II-7-47-2014

Murphy, D. J., Murphy, M. D., O'Brien, B., & O'Donovan, M. (2021). A Review of Precision Technologies for Optimising Pasture Measurement on Irish Grassland. *Agriculture*, *11*(7), 600. https://doi.org/10.3390/agriculture11070600

Mutanga, O., Adam, E., & Cho, M. A. (2012). High density biomass estimation for wetland vegetation using WorldView-2 imagery and random forest regression algorithm. *International Journal of Applied Earth Observation and Geoinformation*, *18*, 399–406. https://doi.org/10.1016/j.jag.2012.03.012

Nickmilder, C., Tedde, A., Dufrasne, I., Lessire, F., Tychon, B., Curnel, Y., Bindelle, J., & Soyeurt, H. (2021). Development of Machine Learning Models to Predict Compressed Sward Height in Walloon Pastures Based on Sentinel-1, Sentinel-2 and Meteorological

Data Using Multiple Data Transformations. *Remote Sensing*, *13*(3), 408. https://doi.org/10.3390/rs13030408

Obanawa, H., Yoshitoshi, R., Watanabe, N., & Sakanoue, S. (2020). Portable LiDAR-Based Method for Improvement of Grass Height Measurement Accuracy: Comparison with SfM Methods. *Sensors*, *20*(17), 4809. https://doi.org/10.3390/s20174809

O'Mara, F. P. (2012). The role of grasslands in food security and climate change. *Annals of Botany*, *110*(6), 1263–1270. https://doi.org/10.1093/aob/mcs209

Otgonbayar, M., Atzberger, C., Chambers, J., & Damdinsuren, A. (2019). Mapping pasture biomass in Mongolia using Partial Least Squares, Random Forest regression and Landsat 8 imagery. *International Journal of Remote Sensing*, *40*(8), 3204–3226. https://doi.org/10.1080/01431161.2018.1541110

Pereira, M., De Almeida, R. G., Macedo, M. C. M., Dos Santos, V. A. C., Gamarra, E. L., Castro-Montoya, J., Lempp, B., & Morais, M. D. G. (2021). Anatomical and nutritional characteristics of *Megathyrsus maximus* genotypes under a silvopastoral system. *Tropical Grasslands-Forrajes Tropicales*, *9*(2), 159–170. https://doi.org/10.17138/tgft(9)159-170

Pezzopane, J. R. M., Bernardi, A. C. de C., Bosi, C., Crippa, P. H., Santos, P. M., & Nardachione, E. C. (2019). Assessment of Piatã palisadegrass forage mass in integrated livestock production systems using a proximal canopy reflectance sensor. *European Journal of Agronomy*, *103*, 130–139. https://doi.org/10.1016/j.eja.2018.12.005

Punalekar, S. M., Verhoef, A., Quaife, T. L., Humphries, D., Bermingham, L., & Reynolds, C. K. (2018). Application of Sentinel-2A data for pasture biomass monitoring using a physically based radiative transfer model. *Remote Sensing of Environment*, *218*, 207–220. https://doi.org/10.1016/j.rse.2018.09.028

Reinermann, S., Asam, S., & Kuenzer, C. (2020). Remote Sensing of Grassland Production and

Management—A Review. *Remote Sensing*, *12*(12), 1949. https://doi.org/10.3390/rs12121949

Richter, K., Atzberger, C., Hank, T. B., & Mauser, W. (2012). Derivation of biophysical features from Earth observation data: Validation and statistical measures. *Journal of Applied Remote Sensing*, *6*(1), 063557–1. https://doi.org/10.1117/1.JRS.6.063557

Tiscornia, G., Baethgen, W., Ruggia, A., Do Carmo, M., & Ceccato, P. (2019). Can we Monitor Height of Native Grasslands in Uruguay with Earth Observation? *Remote Sensing*, *11*(15), 1801. https://doi.org/10.3390/rs11151801

Tong, X., Duan, L., Liu, T., & Singh, V. P. (2019). Combined use of in situ hyperspectral vegetation indices for estimating pasture biomass at peak productive period for harvest decision. *Precision Agriculture*, *20*(3), 477–495. https://doi.org/10.1007/s11119-018-9592-3

Vázquez-Arellano, M., Griepentrog, H., Reiser, D., & Paraforos, D. (2016). Correction: Vázquez-Arellano, M., et al. 3-D Imaging Systems for Agricultural Applications—A Review. Sensors 2016, 16, 618. *Sensors*, *16*(7), 1039. https://doi.org/10.3390/s16071039

Wang, J., Xiao, X., Bajgain, R., Starks, P., Steiner, J., Doughty, R. B., & Chang, Q. (2019). Estimating leaf area index and aboveground biomass of grazing pastures using Sentinel-1, Sentinel-2 and Landsat images. *ISPRS Journal of Photogrammetry and Remote Sensing*, *154*, 189–201. https://doi.org/10.1016/j.isprsjprs.2019.06.007

Wang, Y., Wu, G., Deng, L., Tang, Z., Wang, K., Sun, W., & Shangguan, Z. (2017). Prediction of aboveground grassland biomass on the Loess Plateau, China, using a random forest algorithm. *Scientific Reports*, *7*(1), 6940. https://doi.org/10.1038/s41598-017-07197-6

Zhang, H., Sun, Y., Chang, L., Qin, Y., Chen, J., Qin, Y., Du, J., Yi, S., & Wang, Y. (2018). Estimation of Grassland Canopy Height and Aboveground Biomass at the Quadrat Scale

Using Unmanned Aerial Vehicle. *Remote Sensing*, *10*(6), 851. https://doi.org/10.3390/rs10060851

Supporting information

S1 The main vegetation indices from literature calculated and respective references

VI	Equation	Reference
ARVI	NIR – RED – (BLUE – RED) / NIR + RED - (BLUE - RED)	Kaufman & Tanre, 1992
CI_{Green}	NIR / (GREEN – 1)	Gitelson *et al*., 2003
CI_{RE}	NIR / (RE – 1)	Gitelson *et al*., 2003
CVI	NIR × (RED / $GREEN^2$)	Vincini *et al*., 2008
DVI	NIR – RED / 32767.5	Richardson & Wiegand, 1977
EVI	2.5 × ((NIR – RED) / (NIR + 6 × RED - 7.5 × BLUE + 1))	Huete *et al*.,1997
GNDVI	(NIR – GREEN) / (NIR + GREEN)	Gitelson *et al*., 1996
GRVI	GREEN – RED / GREEN + RED	Sripada *et al*., 2006
IRG	RED – GREEN / 32767.5	Gamon & Surfus, 1999
LCI	(NIR – RED) / (NIR – RED)	Datt *et al*., 1999
MSR	(NIR / RED – 1) / ((NIR / RED) $^{0.5}$ + 1)	Chen, 1996
NDVI	(NIR – RED) / (NIR + RED)	Rouse *et al*., 1973
NDVIRE	(NIR – RE) / (NIR – RE)	Gitelson *et al*., 2003
NGRDI	(GREEN – RED) / (GREEN + RED)	Tucker, 1979
PRI	BLUE – GREEN / RED + GREEN	Gamon *et al*., 1992
RDVI	(NIR – RED) / $(NIR + RED)^{0.5}$	Reujean & Breon, 1995
RVI	RED / NIR	Jordan,1969
SIPI	NIR – BLUE / NIR+ BLUE	Penuelas *et al*., 1995
SR	NIR / RED	Birth & McVey, 1968
SRRE	NIR / RE	Gitelson *et al*., 2005
TVI	$((NIR – RED) / (NIR + RED))^{0.5}$ + 0.5	Deering *et al*., 1975
$VARI_{Green}$	(GREEN – RED) / (GREEN + RED + BLUE)	Gitelson et al., 2002
$VARI_{RE}$	(RE – (1.7 × RED) + (0.7 × BLUE)) / (RE + (2.3 × RED) + (1.3 × BLUE))	Gitelson et al., 2002

Abbreviations: RE: Red Edge; NIR: near infrared; ARVI: Atmospherically Resistant Vegetation Index; CIGreen: Chlorophyll Index; CI_{RE}: Chlorophyll Index Rededge; CVI: Chlorophyll Vegetation Index; DVI: Difference Vegetation Index; EVI: Enhanced Vegetation Index; GNDVI: Green Normalized Difference Vegetation Index; GRVI: Green-Red Vegetation Index; IRG: Red-Green Ratio Index; LCI: Leaf Chlorophyll Index; MSR: Modified Simple Ratio; NDVI: Normalized Difference Vegetation Index; NDVIRE: Normalized Difference Red Edge/Red; NGRDI: Normalized Red-Green Difference Index; PRI: Photochemical Reflectance Index; RDVI: Red Green Ratio Index; RVI: Ratio Vegetation Index; SIPI: Structure Insensitive Pigment Index; SR: Simple Ratio; SRRE: Red-Edge Simple Ratio; TVI: Transformed Vegetation Index; VARIgreen: Vegetation Atmospherically Resistant Index and $VARI_{RE}$: Visible Atmospherically Resistant Indices Red Edge

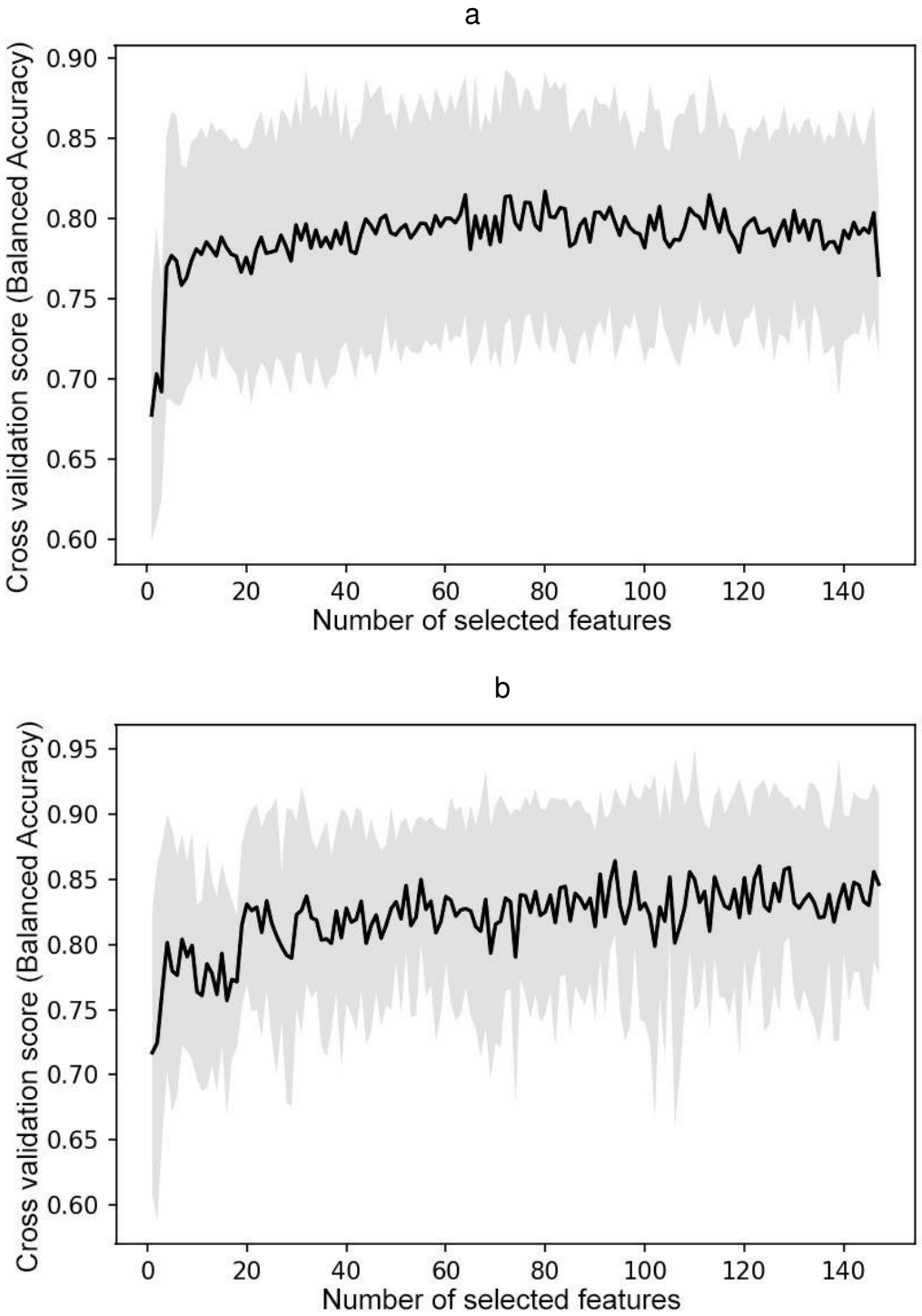

S2 Cross-validation score as a function of the number of features selected for the height classification models using Recursive Feature Elimination in the different DR5 (a) and DR1 (b) intervals respectively.

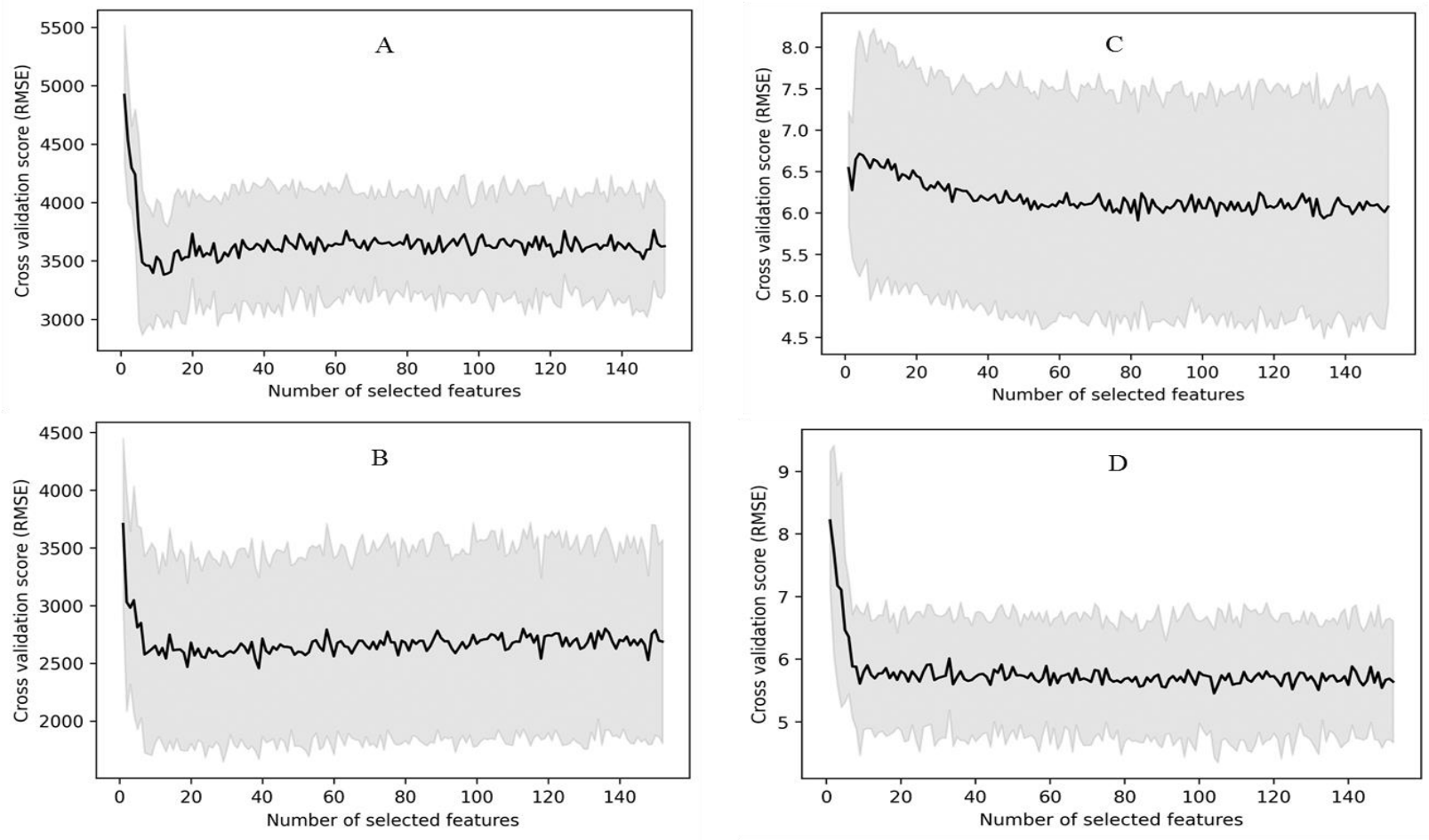

S3 Cross-validation score as a function of the number of variables selected for the prediction models of AFB (A and B) and DMC (C and D) using Recursive Feature Elimination in the different DR5 and DR1 intervals respectively.